www.czasopisma.pan.pl PAN www.journals.pan.pl

Acta Geologica Polonica, Vol. 73 (2023), No. 4, pp. 773–799
DOI: 10.24425/agp.2023.145622

Stratigraphic Emmental: High-resolution allostratigraphy reveals multiple intra-formational unconformities in shallow ramp mudstone: Upper Cretaceous, Western Canada Foreland Basin

ELIZABETH A. HOOPER[1, 2] and A. GUY PLINT[1*]

[1] *Department of Earth Sciences, The University of Western Ontario, London, Ontario, N6A 5B7, Canada; e-mail: gplint@uwo.ca*
[2] *Present address: WSP E&I Canada Limited, 3450 Harvester Road, Suite 100, Burlington, Ontario, L7N 3W5, Canada*
** Corresponding author*

ABSTRACT:

Hooper, E.A. and Plint A.G. 2023. Stratigraphic Emmental: High-resolution allostratigraphy reveals multiple intra-formational unconformities in shallow ramp mudstone: Upper Cretaceous, Western Canada Foreland Basin. *Acta Geologica Polonica*, **73** (4), 773–799. Warszawa.

Marine mudstone of Coniacian age (c. 89.51–86.49 Ma) was deposited on a storm-dominated ramp spanning the foredeep of the Cretaceous Western Canada Foreland Basin. Marine flooding surfaces define 18 allomembers that thin over 300 km, from c. 140 m in the proximal foredeep to c. 20 m close to the forebulge crest. The broadly conformable succession of allomembers is partitioned into five 'tectono-stratigraphic units' by low-angle unconformities that bevel off c. 10 to 20 m of strata over 'arches' that have a length scale of c. 50–100 km and are bounded by relatively linear zones of flexure. Depositional history involved two alternate modes: 'Background' deposition of subtly-tapered allomembers took place on a planar sea floor, subject to regional flexural subsidence, with sea-level modulated by Milankovitch-scale (c. 125 kyr) eustatic cycles. 'Flexural' events deformed the strata into troughs and arches across narrow zones of flexure. Arch crests were bevelled off, probably by submarine wave erosion. Eroded sediment did not accumulate in troughs but was advected beyond the study area by storm-driven processes. Cycles of deposition, warping and erosion were repeated five times on an average timescale of 600 kyr. Arches and troughs do not coincide with Precambrian basement structures, and their origin remains enigmatic. Changes in in-plane stress may have effected the localized vertical motion.

Key words: Allostratigraphy; Upper Cretaceous; Alberta; Foreland Basin; Mudstone; Tectonics.

INTRODUCTION

Historically, mudstone successions have been interpreted to represent relatively slow and continuous deposition in relatively deep, quiet water (Potter *et al.* 1980). More recent work has shown that many 'offshore mudstones' show evidence of deposition from vigorous currents, and that the succession may be punctuated by subtle but extensive disconformities (Schieber 1994, 2016; Macquaker *et al.* 2007; Schieber *et al.* 2007; Plint *et al.* 2012a, 2017; Li and Schieber 2022). Demonstration of stratigraphic hiatuses is particularly effective when borehole data are used, wireline logs are of good quality, and wells are closely spaced. The Western Canada Foreland Basin contains up to c. 4 km of Upper Jurassic, Cretaceous,

Text-fig. 1. Paleogeographic map of western North America for the Middle Coniacian showing the location of the study area in relation to the Interior Seaway. The map shows the generalized position of the shoreline during deposition of the Muskiki Member. The tan shading shows the interpreted maximum regressive extent of the Marshybank Member in the Late Coniacian at the time the CS23 erosion surface formed (after Plint *et al.* 2017; modified from map by R. Blakey, http://cpgeosystems.com).

and Paleocene clastic sediments that form a major petroleum province, thoroughly explored through several hundred thousand boreholes (Wright *et al.* 1994). Both core and wireline log data are publicly-accessible and provide an unparalleled opportunity to make a regional investigation of three-dimensional stratal architecture (based on correlation of flooding surfaces) and facies distribution (based on outcrop, wireline log signature, and limited core).

This study focuses on a c. 100 m thick, mudstone-dominated succession of Coniacian age that was deposited on a shallow marine ramp spanning the foredeep of the Cretaceous foreland basin. The purpose of this paper is to illustrate the internal stratal architecture of the Coniacian mudstone succession, highlight unconformity-bounded packages, and show, in map view, the regions of stratal preservation and hiatus. Without high-resolution physical correlation and mapping of the component allomembers, such stratigraphic complexity would be unrecognizable, particularly because several unconformity-bounded packages commonly lie within a single molluscan biozone. This work illustrates the importance of ***not*** assuming that offshore mudstone successions necessarily preserve a complete record of deposition. This is particularly important if geochemical investigations, such as carbon-isotope stratigraphy, are contemplated for a mudstone succession.

GEOLOGICAL SETTING

Subsidence of the Western Canada Foreland Basin was initiated in the Jurassic as the result of flexure of the cratonic lithosphere under the load of accreted terranes and the tectonically thickened Cordilleran fold-and-thrust belt to the west (Price 1994; Evenchick *et al.* 2007; Miall and Catuneanu 2019; Ricketts 2019). Additional, long wavelength (c. 1000 km) dynamic subsidence was driven by the flow of asthenospheric mantle, driven by the subducting plate (Mitrovica *et al.* 1989; Liu *et al.* 2014; Li and Aschoff 2022). The earliest preserved foreland strata were deposited from the Late Jurassic (Kimmeridgian) to Early Cretaceous (Valanginian), when sediment was supplied to the Canadian portion of the basin by both local rivers and a continent-scale, north-flowing drainage system with headwaters in the south-western and possibly also the south-eastern United States (Williams and Stelck 1975; Wright *et al.* 1994; Raines *et al.* 2013). In the Early Cretaceous (Berriasian to Barremian), diminished tectonic activity in the Rocky Mountain Cordillera resulted in isostatic uplift and erosional truncation of Upper Jurassic to Lower Cretaceous sediments in the foredeep (Leckie and Cheel 1997; Leier and Gehrels 2011). Subsidence resumed in the Aptian, accompanied by gradual marine flooding by a southward-advancing extension of the Polar Ocean. Deltaic and alluvial systems prograded broadly northward, supplied by large river systems that carried sediment from the Canadian Shield, the Appalachians, and the Cordillera (Benyon *et al.* 2014; Blum and Pecha 2014).

At about the Albian–Cenomanian boundary (c. 100.5 Ma), a southward-encroaching embayment of the Polar Ocean (the Mowry Sea), merged with a northward-advancing arm of the proto Gulf of Mexico to form the early Greenhorn Sea (Williams and Stelck 1975). This seaway continued to widen through the Late Cenomanian to a maximum extent in the Early Turonian before progressive eustatic sea-level fall caused narrowing to a minimum in the Late Turonian and earliest Coniacian, as recorded by shallow marine and shoreface sandstones of the Cardium Formation (Nielsen *et al.* 2008; Shank and Plint 2013; Plint *et al.* 2022). A new cycle of relative sea-level rise (a manifestation of the Niobrara Cycle; Kauffman 1977) drowned the earliest Coniacian regressive sandstones, and, in Alberta and British Columbia, drove the shoreline so far to the west that no nearshore deposits are preserved in Foothills outcrop sections (Stott 1963, 1967). Sea-level fall in the Late Coniacian allowed rivers draining the Cordillera to build deltaic systems along the western margin of the basin (Plint and Norris 1991; Text-fig. 1). Another cycle of sea-level rise commenced in latest Coniacian time, continuing through the Early Santonian, leading to widespread deposition of marine mudstone across Alberta and NE British Columbia. This transgression coincided with a period of renewed flexural subsidence of the foreland basin (Nielsen *et al.* 2008; Hu and Plint 2009; Plint *et al.* 2012a). Despite the generally high flexural subsidence rate through the Late Cretaceous, the sedimentation rate was sufficiently high that the sea floor was maintained at a depth of a few tens of meters, allowing storm waves to efficiently redistribute muddy sediment, maintaining a near-planar, wave-graded ramp (Nielsen *et al.* 2008; Varban and Plint 2008; Plint *et al.* 2012b, 2017).

STRATIGRAPHIC SETTING

Lithostratigraphy

This study concerns the Muskiki and Marshybank members of the Wapiabi Formation (Text-fig. 2). The Wapiabi Formation ranges in age from Early Coniacian to Early Campanian and comprises up to about 650 m of marine mudstone. Minor intercalations of sandstone are present in the west, whereas to the east, in south-easternmost Alberta, Saskatchewan and Manitoba, marls and muddy chalks appear, particularly in strata of Santonian age (McNeil 1984; Nielsen *et al.* 2008). Stott (1963, 1967) showed that, throughout the fold-and-thrust belt, the Wapiabi Formation could consistently be divided, on lithostratigraphic grounds, into seven members. Each member was characterized by a distinct suite of lithologies that could be traced along most of the Rocky Mountain Foothills from NE British Columbia (55.30º N) to the Montana border (49º N). The lowest unit is the Muskiki Member that consists primarily of offshore marine mudstone and siltstone and disconformably overlies the Cardium Formation. At outcrop, the boundary between the Muskiki and the overlying Marshybank Member typically forms a rapidly-gradational to sharp contact between mudstone and overlying, intensely bioturbated siltstone and silty sandstone. Towards the north-west, particularly north of the Athabasca River (c. 53º N), the siltstone-dominated Marshybank Member undergoes a lateral facies change to include clean, well-sorted marine sandstone and minor alluvial deposits (Plint and Norris 1991). These sandy facies were originally assigned to the Bad Heart Formation (Stott 1967), although subsequent work (Plint *et al.* 1990)

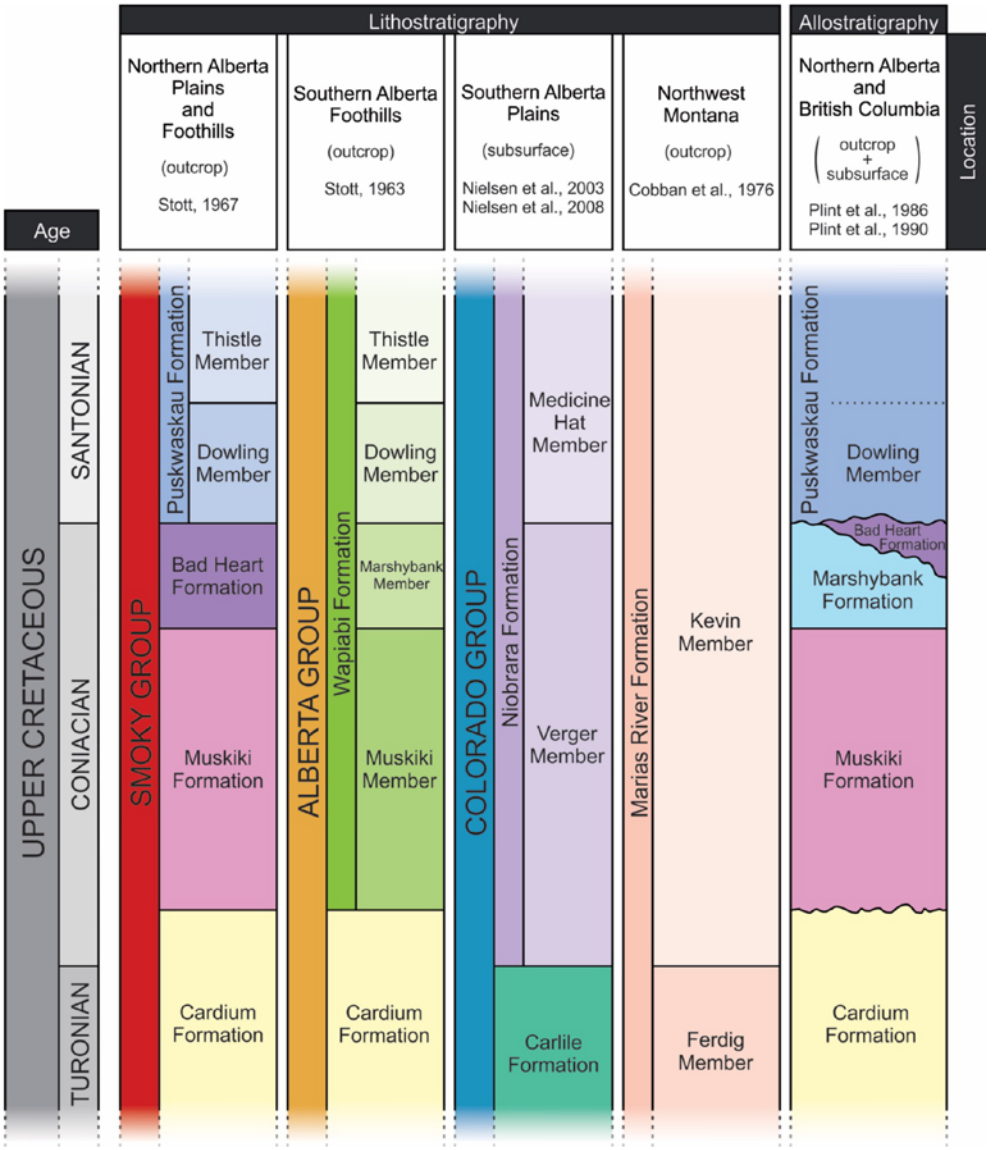

Text-fig. 2. Chart summarizing stratigraphic nomenclature for the Turonian to Santonian strata in regions of western Canada and Montana. See Text-figs 4 and 5 for the stratigraphic distribution of zonal inoceramid species, and geochronological control.

showed that, in the Foothills, the Marshybank and 'Bad Heart' strata were equivalent. The type Bad Heart Formation is confined to the Alberta Plains, is petrologically distinct, and slightly younger than the Marshybank (Plint *et al.* 1990; Donaldson *et al.* 1998, 1999). A change of lithostratigraphic terminology occurs at the Canada-U.S.A. border: rocks of the Cardium and Wapiabi formations in Alberta are broadly correlative with the Ferdig and Kevin members of the Marias River Formation in Montana (Cobban *et al.* 1976; Nielsen *et al.* 2003; Grifi *et al.* 2013; Shank and Plint 2013; Plint *et al.* 2017; Text-fig. 2).

Allostratigraphy

In order to better understand temporal and palaeogeographic relationships during deposition of the Coniacian rocks, an allostratigraphic approach to correlation was employed in a series of linked studies that extend from NE British Columbia to northern Montana (Plint 1990, 1991; Plint *et al.* 1990; Plint and Norris 1991; Grifi 2012; Grifi *et al.* 2013; Hooper 2019). Previous studies are reviewed in Plint *et al.* (2017). The present paper focuses specifically on the study of Hooper (2019) in west-central Alberta (Text-fig. 3).

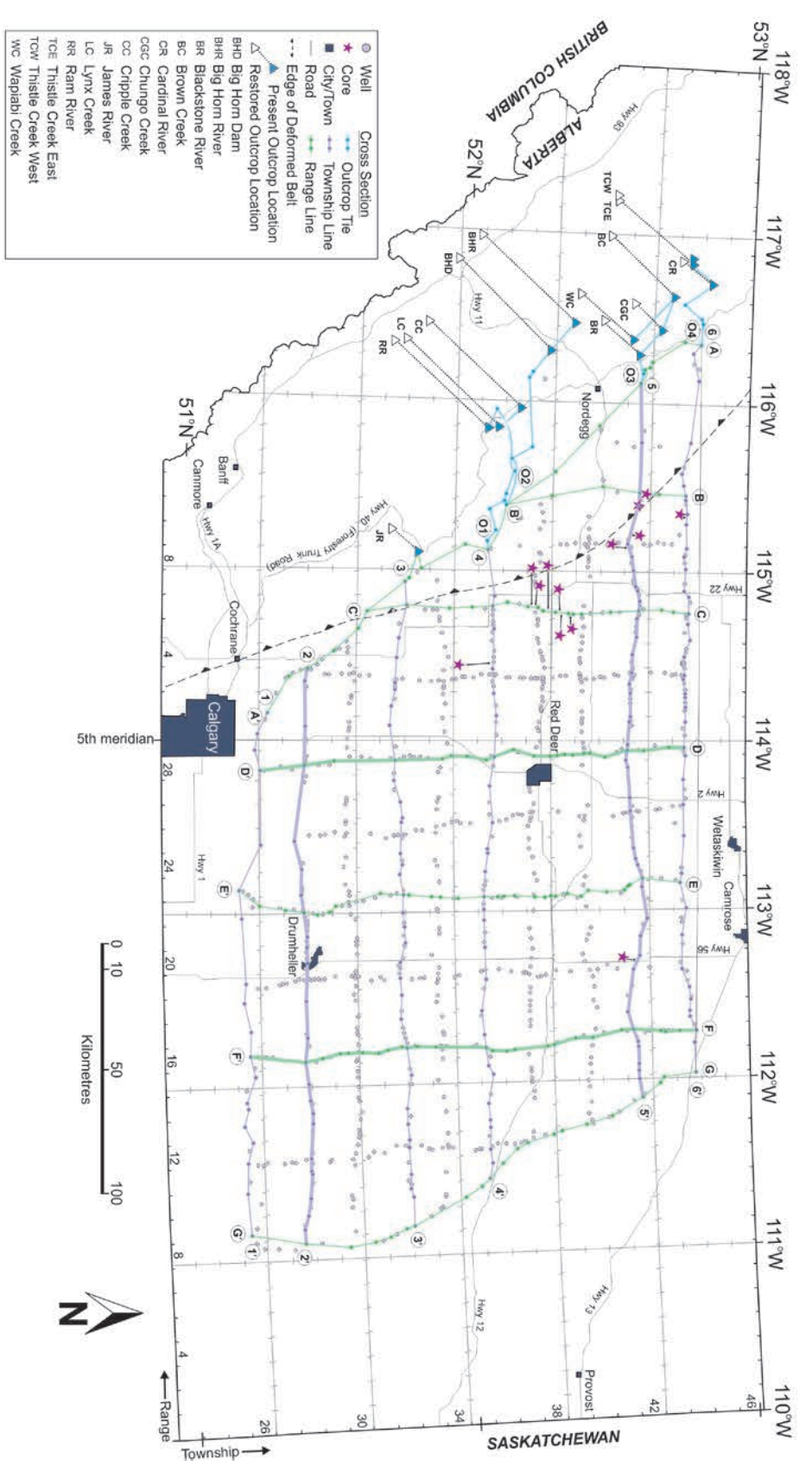

Text-fig. 3. Base map of the study area (located in Text-fig. 1), showing distribution of well, core and outcrop data that form the basis for the study. Note that well locations in Alberta use the Dominion Land Survey grid system of Townships (Twp; north-south) and Ranges (Rge; east-west). The two thick mauve lines represent oblique dip cross-sections in Townships 28 (2-2', Text-fig. 4) and 42 (5-5', Text-fig. 5) whereas the two thick green lines represent oblique strike cross-sections in Ranges 28 (D-D', Text-fig. 6) and 16 (F-F', Text-fig. 7). Outcrop to subsurface correlations on the western margin of the study are given in Plint *et al.* (2017); the present paper focuses primarily on the subsurface data to the east of the study described in Plint *et al.* (2017).

The shallow-marine setting of the Muskiki and Marshybank rocks made them sensitive to even minor relative sea-level changes. In consequence, the rocks comprise stacked, transgressive-regressive successions, typically <10 m thick. The upper surface of each succession is a marine flooding surface or a composite sequence boundary and flooding surface (Plint 1991; Plint *et al.* 2017). Upward-shoaling successions can, therefore, be considered equivalent to parasequences, or small-scale depositional sequences in conventional sequence stratigraphic terms.

Plint *et al.* (2017) presented an allostratigraphic correlation scheme, based on a grid of wireline log cross-sections that linked exposures extending 750 km along strike, from Grande Cache, Alberta, in the north-west, to Kevin, Montana in the south-east. Twenty-four allomembers were defined on the basis of mappable marine flooding surfaces. New collections of ammonites and inoceramid bivalves made in the Foothills outcrop belt were integrated into the physical, allostratigraphic framework, as detailed in Landman *et al.* (2017), Plint *et al.* (2017), and Walaszczyk *et al.* (2017). A critical finding of these allo- and biostratigraphic studies was that, throughout the study area, the first occurrence of specific zonal fossils always coincided with the same marine flooding surface (Text-figs 4 and 5). It was, therefore, concluded that flooding surfaces could be treated as proxy time lines, comparable to biostratigraphic first occurrence datums.

In the subsurface study area of Hooper (2019), 18 allomembers, termed CA1 to CA18, were recognized, bounded by flooding surfaces CS1 to CS17. When correlated farther to the north and west, the Marshybank Member thickens and coarsens, and additional allomembers CA19 to CA24 can be recognized (Plint *et al.* 2017). The top of allomember CA23 is surface CS23 (also termed 'top Marshybank' or 'Tmbk' in Hooper 2019). Surface CS23 is a pebble-veneered, regional erosion surface with up to several tens of meters of relief and marks the maximum regression of the Marshybank Member in the latter part of the Late Coniacian (Plint and Walker 1987; Plint *et al.* 2017). Allomember CA24 records an upward-deepening succession and the upper surface is designated SS0, which marks the first appearance of Santonian fossils. The overlying, mudstone-dominated facies indicate major transgression and shoreline backstep (Plint *et al.* 2017; Text-fig. 2). Surfaces CS23 and SS0 can be traced eastward into the Plains, although SS0 becomes increasingly subtle and difficult to recognize, and in places merges with CS23.

Integration of allostratigraphy, biostratigraphy, carbon-isotope stratigraphy, and geochronology suggests that the E7 surface at the base of the studied succession has an age of 89.51 Ma whereas the Coniacian–Santonian boundary is at 86.49 Ma, implying that the studied interval spans close to 3 Myr (Plint *et al.* 2017; Text-figs 4 and 5).

STUDY AREA, DATA, AND METHODS

The study area is located in west-central Alberta and embraces about 45,000 km^2, extending c. 180 km north-south and c. 300 km east-west (Text-fig. 3). The western margin of the area lies within the Foothills fold and thrust belt, where 13 partial or complete outcrop sections were examined. Each outcrop section was palinspastically restored using the bed length method of Dahlstrom (1969), based on the most recent cross-sections provided in geological maps compiled by the Geological Survey of Canada (details in Hooper 2019). In the adjacent subsurface, 1020 paired gamma-ray and resistivity logs (average well spacing of 3.5 km) were used to construct 13 cross-sections oriented broadly north-south, and ten sections oriented east-west (Text-fig. 3). Because the Muskiki and Marshybank strata are generally non-reservoir, core is scarce. However, fourteen cores that penetrate all or part of the studied interval were identified, logged and photographed.

Each outcrop section was logged in detail, with particular attention to lithology, sedimentary structures, trace fossils, and the nature of facies transitions. An Exploranium GR-130 ® spectrometer was used to make gamma-ray profiles for nine of the most complete sections. Readings were typically 1 m apart, but closer in intervals of abrupt facies change. Each station was counted for 30 seconds, and total gamma ray, potassium, uranium, and thorium counts were recorded. The gamma ray data provided a sensitive measure of (sometimes invisible) lithological variation and greatly improved the confidence with which outcrop sections could be correlated to wireline logs.

Well logs were correlated on the basis of allostratigraphic principles, where allostratigraphic units are defined by bounding surfaces rather than lithology (North American Commission on Stratigraphic Nomenclature 2005). In this case, bounding surfaces comprise marine flooding surfaces or composite subaerial unconformities and marine flooding surfaces. In wireline logs, flooding surfaces were identified at horizons across which there was an abrupt increase in gamma-ray and decrease in resistivity values, cor-

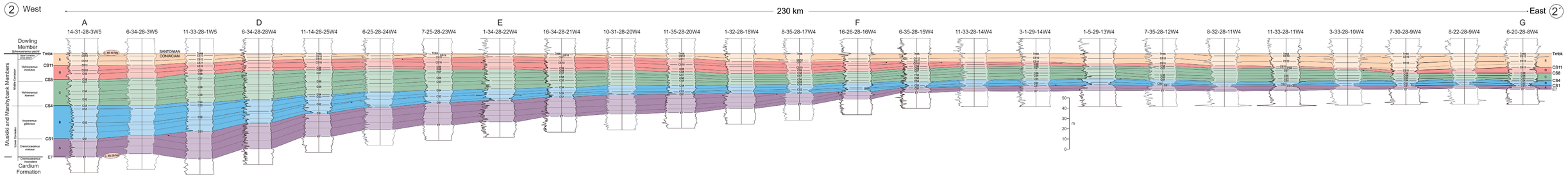

Text-fig. 4. East-west cross-section (230 km long; gamma ray log on left, resistivity log on right) in Twp 28. The E7 surface separates the Cardium Formation from the Muskiki Member (Plint *et al.* 1986) and 'Tmbk' indicates the maximum regressive surface at, or close to the Coniacian–Santonian boundary. Cores show that the entire succession comprises mudstone or siltstone with very minor fine sandstone. Allomembers are bounded by flooding surfaces labeled 'CS' (= Coniacian Surface). Colour coding used in this and Text-figs 5-7, 9-13, 16 and 17) identifies tectono-stratigraphic units A to E that comprise packages of allomembers that are defined by erosion surfaces CS1, CS4, CS8, CS11 and Tmbk.

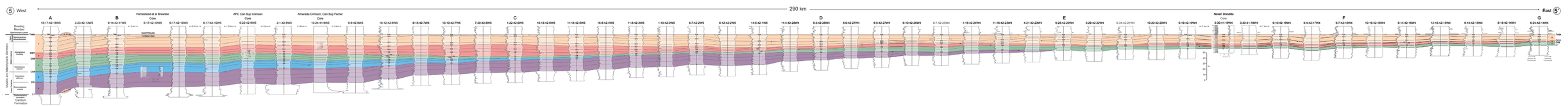

Text-fig. 5. East-west cross-section (290 km long) in Twp 42. Note both thinning and thickening of colour-coded tectono-stratigraphic units A to E (particularly unit E) towards the east.

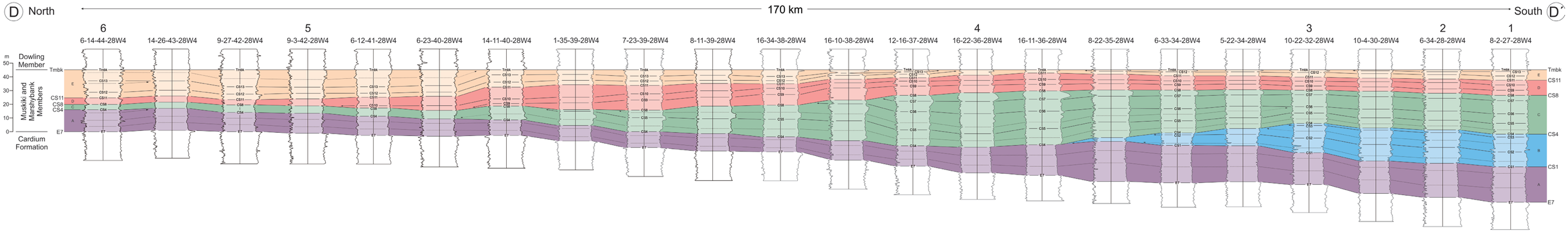

Text-fig. 6. North-south log cross-section (170 km long) in Rge 28. Tectono-stratigraphic units C and D show marked erosional truncation from south to north whereas a greater thickness of units D and E is preserved in the area where units B and C have been removed.

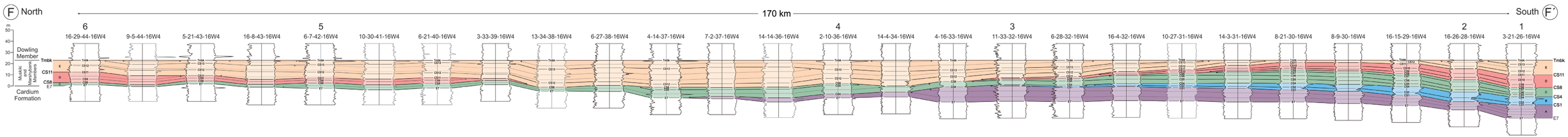

Text-fig. 7. North-south log cross-section (170 km long) in Rge 16. All tectono-stratigraphic units are thinner in this more distal part of the foredeep, and all units are erosionally truncated from south to north. Unit E in particular shows marked thinning and thickening across broad arches and basins.

responding to an abrupt increase in the clay content of the sediment. This interpretation was confirmed by observation of abrupt facies changes in cores, and through correlation to outcrop.

Allomembers were defined at surfaces that were consistently mappable for hundreds of kilometers. Less extensive upward-shoaling successions aided correlation on a local basis. Allomember-bounding surfaces were correlated throughout the grid of cross sections, each surface being 'looped' through east-west and north-south lines to ensure consistent correlation. The subtle flooding surface SS0, which marks the Coniacian–Santonian boundary in outcrop (Plint *et al.* 2017), is not easily recognized in well logs and hence, for practical purposes, the slightly lower, more prominent, maximum regressive surface (surface CS23 of Plint *et al.* 2017) was used as the datum for all cross-sections. In the cross-sections presented herein, the maximum regressive surface is used as the datum in all cross-sections and is labeled 'Tmbk' ('top Marshybank').

Ammonites and inoceramid bivalves were collected in all the studied outcrop sections, and details of their distribution are given in Landman *et al.* (2017), Plint *et al.* (2017), and Walaszczyk *et al.* (2017). Specific zonal species appeared consistently above the same marine flooding surface throughout the study area. The first appearance levels for each species of zonal inoceramid are shown on the western end of Text-figs 4 and 5, based on correlation of outcrop sections to the nearest wireline log (Plint *et al.* 2017). Although ammonite and bivalve fragments were noted in cores, none were sufficiently complete to allow specific identification. In consequence, the extent of biozones in subsurface is *inferred*, based on the detailed correlation of flooding surfaces (Text-figs 4–7).

Isopach values were measured from well logs and rounded to the nearest meter. Isopach maps were made with the SURFER® program using the default kriging algorithm to create a regular grid (grid cell size = 0.05º × 0.05º) from the randomly-distributed thickness values in the database. Each isopach map generated in SURFER® was imported into CorelDRAW ® and superimposed on the study area base map. Minor manual editing of contours removed geologically unreasonable isopach patterns and minor bull's eyes. Isolines were manually extrapolated into the deformed belt based on the thickness of units measured in palinspastically-restored outcrop sections. Because data density in the Foothills is low, isolines were plotted as broken lines, signifying a lower level of confidence.

RESULTS

Stratal Geometry

From the 23 well-log cross-sections in Hooper (2019), four representative sections were chosen to illustrate the allomember-scale stratigraphy of the Muskiki and Marshybank strata in east-west (Text-figs 4 and 5) and north-south (Text-figs 6 and 7) views. Allomembers have distinctive log signatures that can be correlated throughout the grid of cross-sections. This property forms the basis for the results presented below. The base of the Muskiki Member is defined by surface E7 that erosionally truncates the Cardium Formation (Wadsworth and Walker 1991). The Muskiki and Marshybank members in subsurface are dominated by mudstone and siltstone organized in meter-scale, upward-coarsening successions. Sedimentological and stratigraphic evidence (summarized in Plint *et al.* 2017) suggest that the sediment was deposited on a storm-dominated, low-gradient, shallow-marine ramp. The lack of clinoform physiography is attributed primarily to very efficient, storm-driven dispersal of fine-grained sediment across the ramp, filling accommodation to the top of the 'mud accommodation envelope', defined by ambient wave energy (cf. Varban and Plint 2008; Plint *et al.* 2017).

In the dip-oblique view, allomembers typically show very gradual *depositional thinning* towards the east, away from the foredeep; however subtle to more marked *erosional* beveling and truncation is also recognizable (Text-figs 4, 5). In the north-south (strike-oblique) view (Text-figs 6, 7), there are dramatic changes in the thickness of allomembers. As a result of the detailed correlation of allomembers throughout the grid of cross-sections, it became evident that much of the thickness change seen in the cross-sections is the result of subtle *erosional beveling* on five specific surfaces: CS1, CS4, CS8, CS11, and Tmbk. These subtle unconformities partition the succession into five 'tectono-stratigraphic' units, labelled A through E (Text-figs 4–7).

Isopach maps and biostratigraphy

In order to better illustrate the regional geometry of the Muskiki and Marshybank strata between the E7 and CS23 (Tmbk) surfaces, the isopach data from Hooper (2019; Townships 26–44) were combined with results from the companion study of Grifi (2012; Townships 1–26) immediately to the south. Collectively, these data illustrate some 3 myr of foredeep subsidence extending 450 km in strike and up to

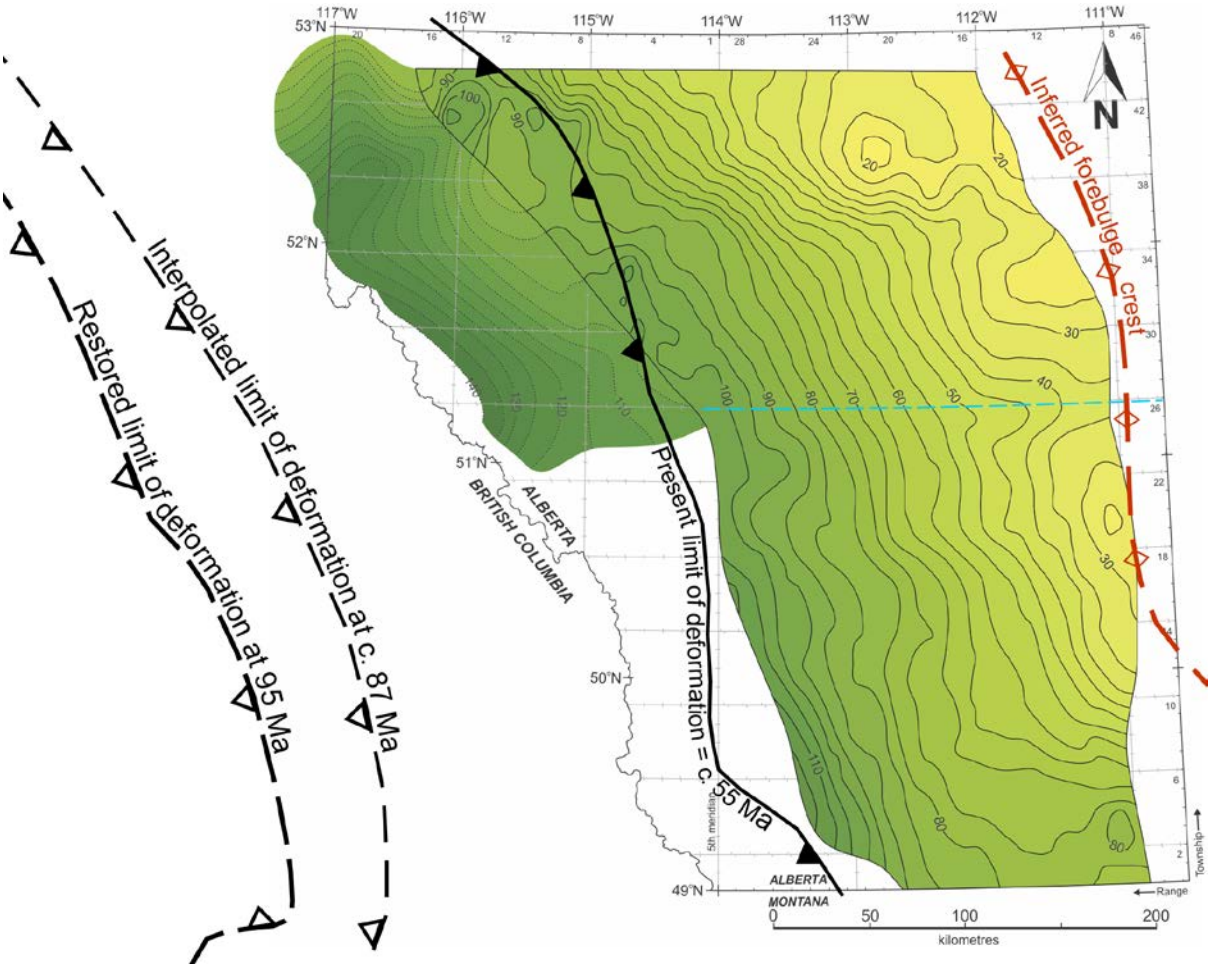

Text-fig. 8. Regional isopach map of SW Alberta showing the total thickness of the Muskiki and Marshybank members, incorporating data from Grifi (2012) south of blue line, and Hooper (2019) north of blue line, for a total of 1730 wells. In Hooper's study area, isolines are extended westward to include thickness data from palinspastically restored outcrop sections. The broken red line indicates the inferred forebulge crest. The restored limit of deformation at 95 Ma and the present limit of deformation (which ceased about 55 Ma) are from McMechan and Thompson (1993). An interpolated deformation limit for 87 Ma (i.e., Late Coniacian) has been added, assuming a linear rate of thrust-front advance. These data suggest that the flexural wavelength of the foredeep was about 400 km, and that, viewed over a 3 Myr timespan, flexural subsidence was relatively uniform across the foredeep.

280 km in dip directions (Text-fig. 8). Text-fig. 8 portrays a wedge of mudstone-dominated sediment that thickens from c. 20 m in the northeast to a maximum of 143 m in outcrop in the west. The position of the Late Coniacian forebulge crest is inferred from the isopach pattern; the corresponding limit of the coeval (c. 87 Ma) deformation front is interpolated from the 95 Ma structural restoration of McMechan and Thompson (1993). These data suggest that, viewed on a c. 3 myr timescale, flexural subsidence of the foredeep was relatively uniform, with a flexural wavelength of c. 400 km. This value is comparable to that determined in other parts of the foredeep (Plint *et al.* 2012a).

The apparently simple pattern of subsidence portrayed in Text-fig. 8 breaks down when the five tectono-stratigraphic units, each spanning an average of c. 600 kyr, are isopached as separate entities (Text-figs 9–13). At this finer level of stratigraphic resolution, a complex pattern of thickness change, deformation, and erosion is revealed. In addition to showing the physical stratigraphy, Text-figs 9–13 show the ranges of the principal zonal inoceramid species, based on Plint *et al.* (2017, 2022). Collectively, the physical and biostratigraphic information in Text-figs 9–13 illustrates the pervasive development of hiatuses and, by implication, anomalous faunal juxtapositions in the stratigraphic record. Were it not for the regional stratigraphic pic-

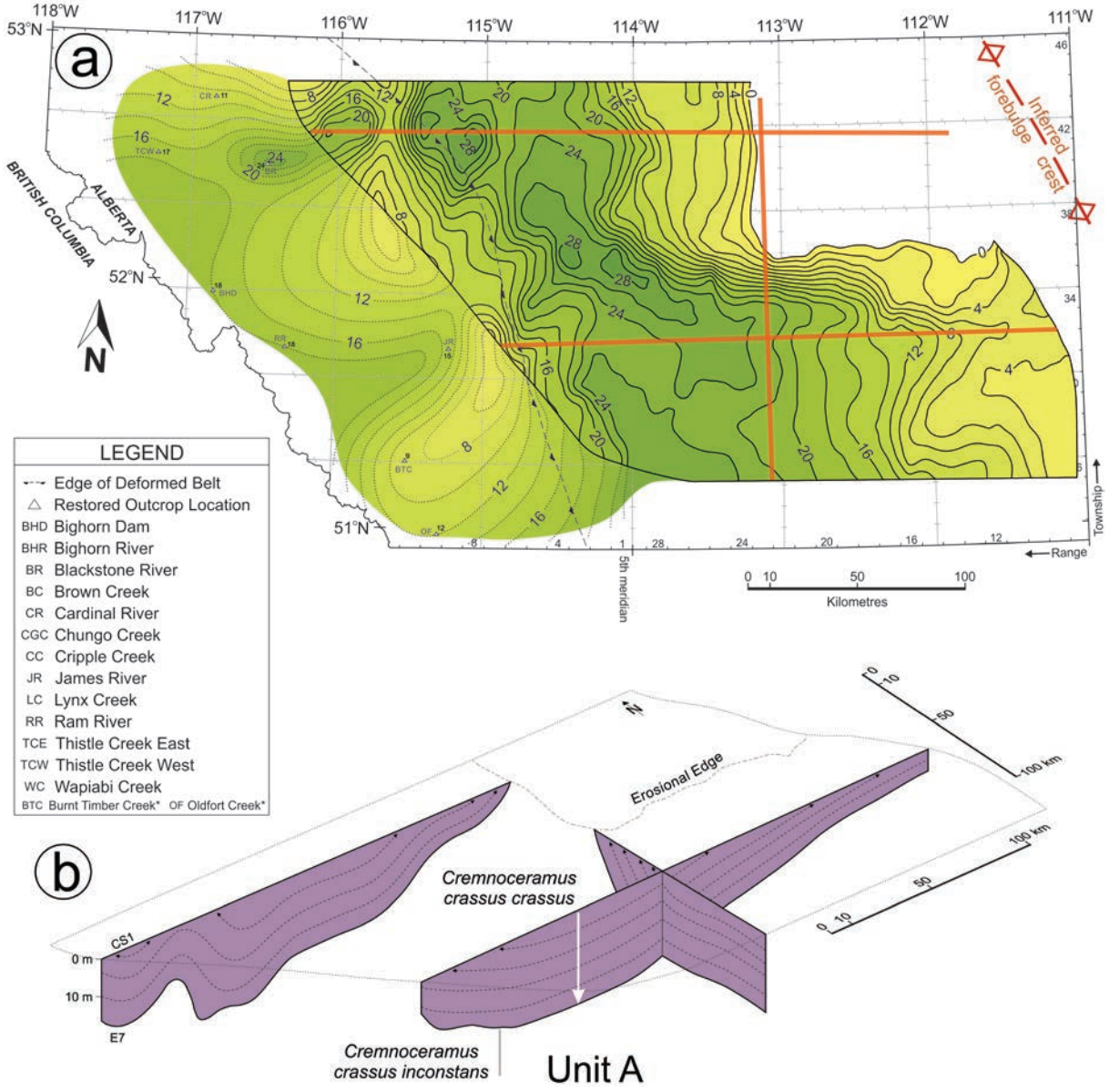

Text-fig. 9. Isopach map and cross-sections of unit A. A – The unit has been completely eroded away in a sub-rectangular area in the north-east. B – Cross-sections (to scale) along the three orange lines in A show that removal of unit A is due primarily to up-arching of the strata and subsequent erosion on surface CS1. In this and Text-figs 10–13, the stratigraphic range of the principal zonal species of inoceramid bivalve are shown (after Plint *et al.* 2017, 2022), with an arrow-head indicating the first (and if applicable, last) appearance of the species. The interpreted position of a portion of the crest of the forebulge (taken from Text-fig. 8) is shown in the north-east.

ture, such as presented here, a study of randomly located stratigraphic sections (cores, outcrops) may easily overlook the cryptic mud-on-mud unconformities. For example, three cores included in Text-fig. 5 sample erosion surfaces CS1, CS8 and CS11 yet none of these surfaces have a lag deposit, and each might be interpreted, if viewed out of regional stratigraphic context, as simply a 'flooding surface'.

Unit A, between E7 and CS1, has a major, north-west-southeast trending depocentre in the central region of the study area (Text-fig. 9A). Within this depocentre, unit A can reach a thickness of 28 m. To the west, unit A thins to 6 m with a minor depocentre at approximately Township 42. In the north-east corner of the study area, unit A is absent over an area of 110 × 80 km. Although internal surfaces within

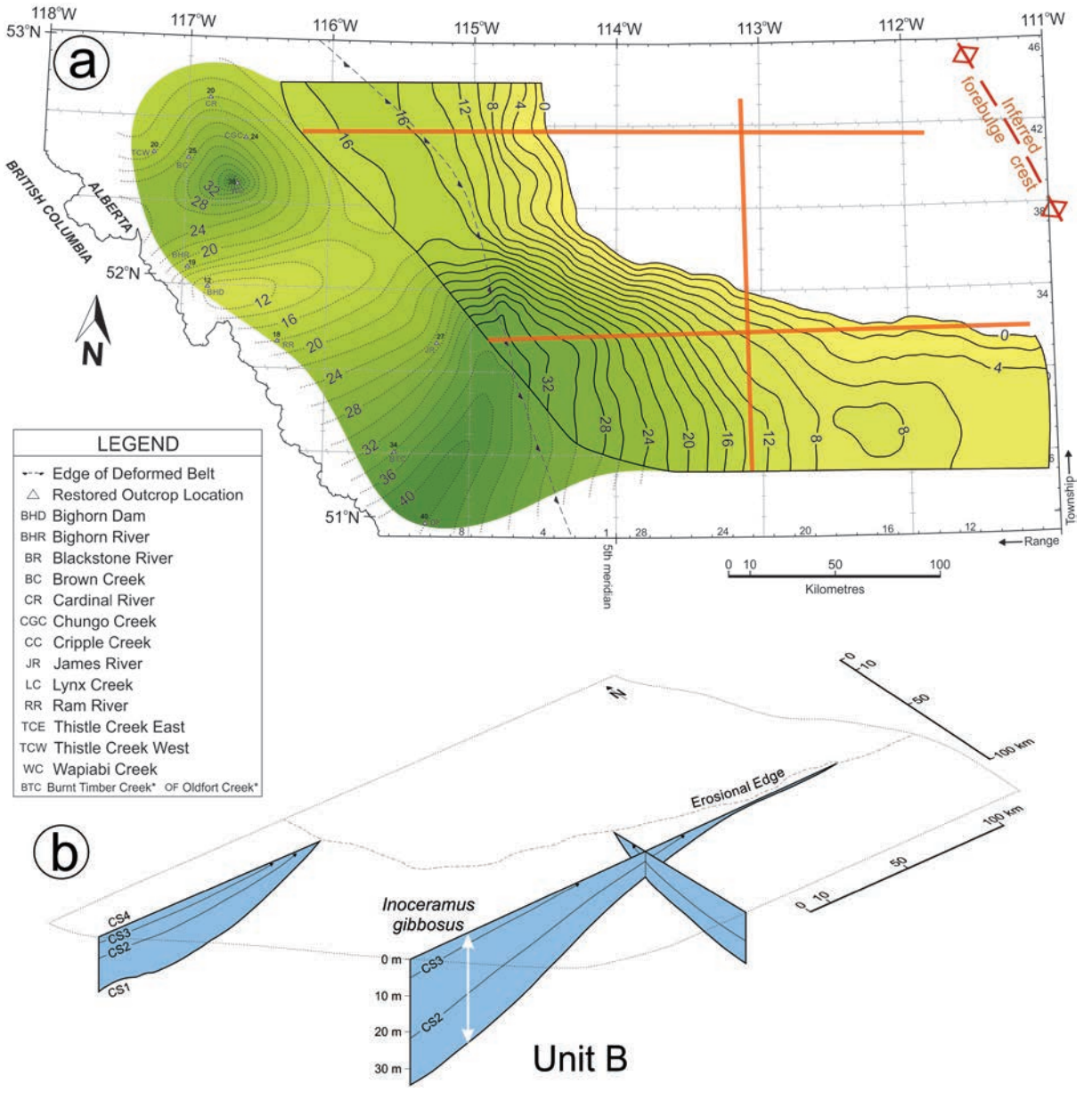

Text-fig. 10. Isopach map and cross-sections of unit B. A – The unit has been eroded away over a large area in the north-east part of the study area as a result of erosion on surface CS4. The western part of the foredeep also appears to be partitioned into two broad 'troughs' separated by an arch at about 52ºN. B – Cross-sections show that unit B thins to the north-east as a result of both depositional thinning and erosion on surface CS4.

unit A show minor depositional thinning towards the east, the primary reason for thinning appears to be due to the arching of stratal surfaces towards the east and north, in which direction they are bevelled off at surface CS1 (Text-fig. 9B).

Unit B, between CS1 and CS4, forms a broad wedge with a principal depocentre up to 40 m thick in the southwest and a minor depocentre in the northwest (Text-fig. 10A). In the north-east, unit B is absent over an area of 200 × 120 km. The removal of unit B appears to be due, in part, to depositional thinning, but seems largely due to erosional truncation on surface CS4 (Text-fig. 10B).

Unit C, between CS4 and CS8, shows an irregular pattern of thickening with a south-western depocentre up to 40 m thick in the Foothills, and a second, east-west elongate depocentre up to 38 m thick, centred on Township 37, adjacent to which there is

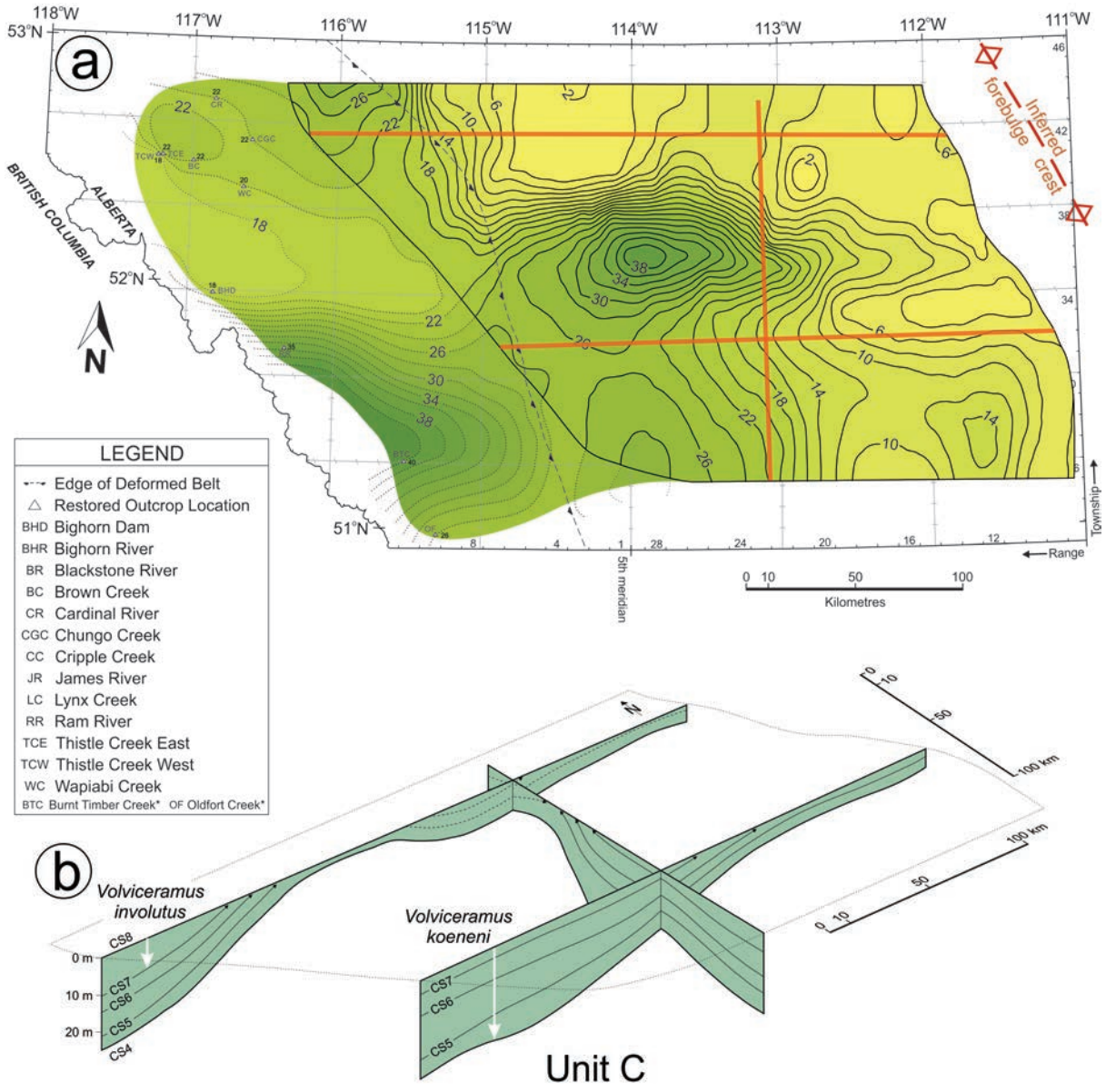

Text-fig. 11. Isopach map and cross-sections of unit C. A – The unit is preserved in an east-west elongate trough across the centre of the study area, flanked by arches to the north and south. The foredeep shows a broad trough in the SE and an arch in the NW. B – Cross-sections show that thinning of unit C is due to both depositional thinning and subsequently, to erosion on CS8 in response to post-depositional arching.

pronounced thinning to the north and south (Text-fig. 11A). Thickening appears to be due to stratal preservation in subtle troughs, whereas thinning is due to truncation on surface CS8 over intervening arches (Text-fig. 11B).

Unit D, between CS8 and CS11, has an isopach pattern unlike that of underlying units A–C in that it does not form a clear, westward-thickening wedge. Instead, unit D comprises several regions of subtle thickening and thinning where the thickness does not exceed 20 m (Text-fig. 12A). Unit D is absent over an area of c. 5,550 km^2 in the eastern part of the study area. This region of *thinning* coincides, in part, with the east-west elongate region of *thickening* in the underlying unit C. The stratal geometry (Text-fig. 12B) suggests that unit D is deformed into a series of subtle troughs and arches, the crests of the arches being eroded on surface CS11.

Unit E, between surface CS11 and Tmbk shows a pronounced wedge-shaped depocentre in the Foothills,

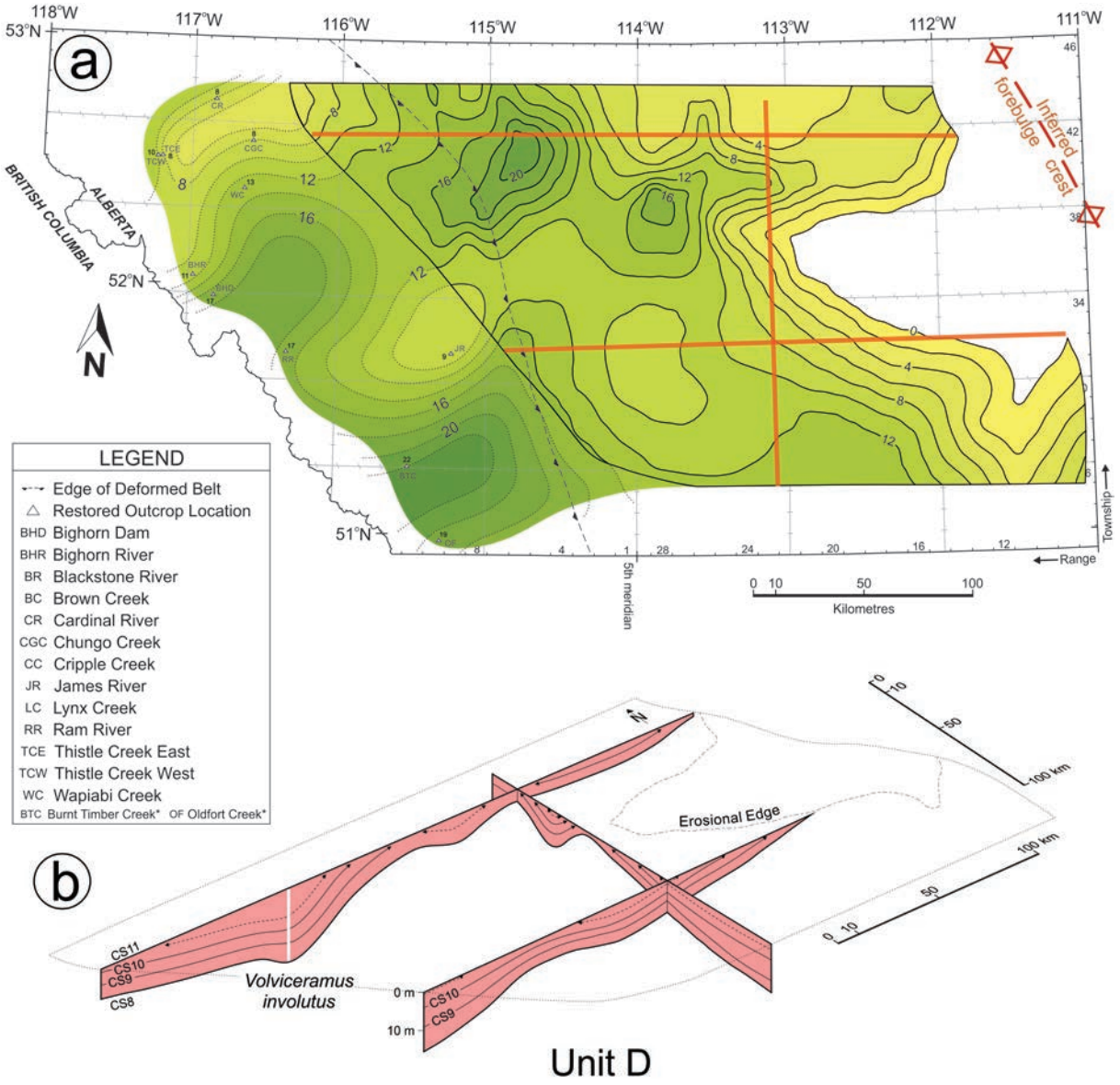

Text-fig. 12. Isopach map and cross-sections of unit D. A – The unit has been erosionally removed in the east, in an area approximately aligned with the elongate thick region in unit C. B – Cross-sections show that thinning and disappearance of unit D is due mainly to erosion on CS11.

up to 65 m thick in the far west. However, to the east of the deformed belt, this simple pattern is replaced by localized regions of thinning and thickening (Text-fig. 13A). Thickened troughs exist in the north-west and east but are separated by broad arches, the tops of which are truncated by surface Tmbk (Text-fig. 13B).

CONTROLS ON SEDIMENTATION

The studied succession of Coniacian strata span about three million years. During that time, five tectono-stratigraphic units, A to E, with an average duration of c. 600 kyr, show that specific regions within the study area experienced temporally-discrete episodes of subsidence and uplift (Text-fig. 14). The spatial changes in unit thickness are interpreted to be the result of a combination of tectonic and eustatic processes that affected sediment dispersal, accommodation, and erosion. This section will discuss the influence of regional flexural subsidence, local tectonic structures, and eustatic sea-level change in producing the observed depositional patterns.

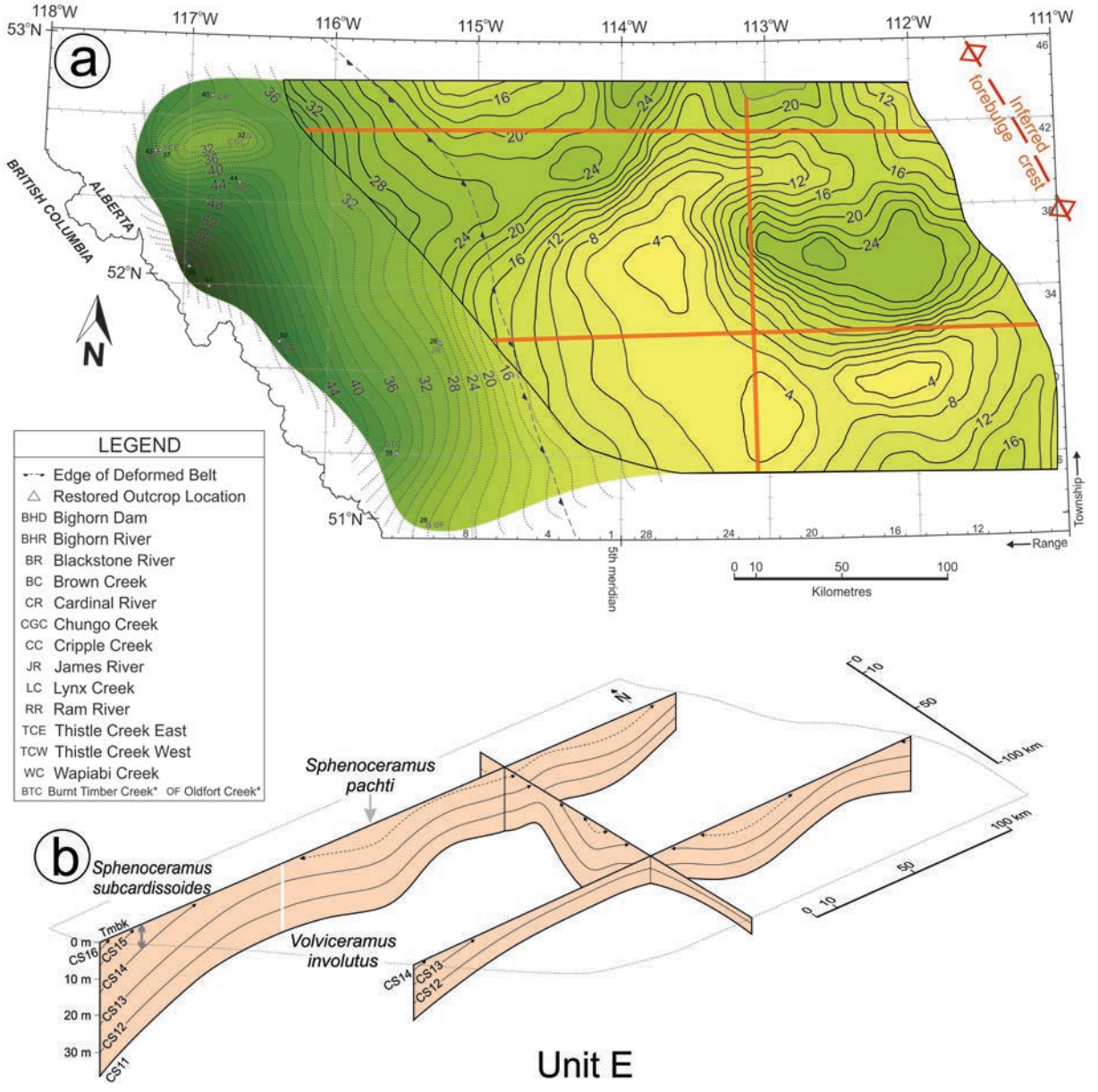

Text-fig. 13. Isopach map and cross-sections of unit E. A – There is a broadly reciprocal pattern relative to unit D, where troughs become arches and vice-versa. Unlike underlying units, unit E shows a pronounced and strike-consistent thickening into the foredeep suggestive of widespread flexural loading. If this is the case, the response of the more distal (eastern) part of the basin is very non-uniform. B – Cross-sections show little syn-depositional thinning of allomembers, suggesting that most thickness changes are due to post-depositional warping and erosion.

Flexural subsidence

The south-westward stratal thickening shown by the total isopach map (Text-fig. 8) is readily explained in terms of regional flexural subsidence, driven primarily by the static load of the accretionary tectonic wedge to the south-west (Jordan and Flemings 1991; Beaumont *et al.* 1993; Evenchick *et al.* 2007). The crest of the Late Coniacian forebulge can be inferred to lie a short distance to the north-east of the studied area, and the contemporaneous (c. 87 Ma) fold and thrust belt lay some 400 km to the south-west (Text-fig. 8). If the structural reconstruction in Text-fig. 8 is correct, the Coniacian deformation front lay about 100 km to the SW of the limit of our isopach data. This data gap introduces some uncertainty regarding the interpretation of possible linkage between activity in the deformed

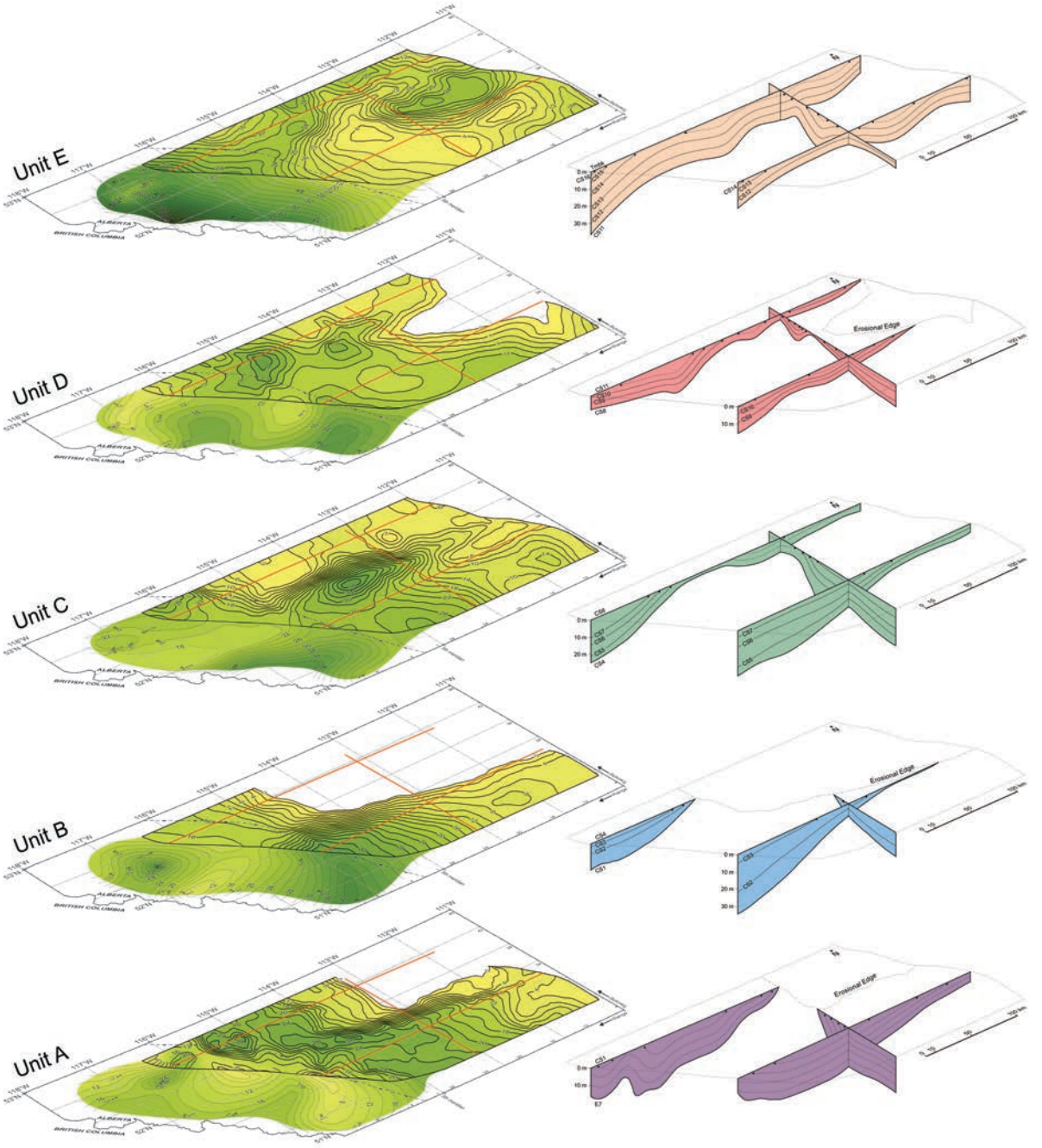

Text-fig. 14. Stacked collation of isopach maps and cross-sections for units A to E to facilitate comparison of the evolving arches and troughs.

belt and the contemporaneous subsidence pattern in the foredeep.

Although tectono-stratigraphic units A–E all show some degree of thickening towards the southwest, this pattern is most consistent in unit E. In units A to D, the *western* part of the study area, mostly west of well control, appears (on admittedly sparse outcrop data), to be divided into a series of arches and troughs on a strike length scale of c. 100–200 km (Text-figs 9–13). The arches and troughs have a reciprocal organization: over time, arches become troughs and vice-versa, such that *cumulative thickness* (Text-fig. 8) appears to reflect spatially uniform subsidence along the western margin of the basin.

A similar pattern of along-strike variation in the magnitude of subsidence in the proximal foredeep has been noted in several other studies of the Western Canada Cretaceous foredeep (Roca *et al.* 2008; Hu and Plint 2009; Plint *et al.* 2012a, 2017, 2018; Grifi *et al.* 2013; Buckley *et al.* 2016). In these examples, depocentres along the western part of the foredeep subsided for c. 200 kyr to 800 kyr before being replaced, typically across a single marine flooding surface (i.e., 'geologically instantaneously'), by a new depocentre located several hundred kilometers along strike. Comparable abrupt changes in along-strike subsidence were documented from Carboniferous strata in the Black Warrior foreland basin in the SE United States (Mars and Thomas 1999). The foregoing studies postulated that this pattern of subsidence was the result of localized loading in front of actively-thickening segments of the deformed belt. This interpretation is supported by modeling and field observations (Marshak *et al.* 1992; Macedo and Marshak 1999), which showed that arcuate salients in a deformation front could develop where the fold and thrust belt was partitioned by strike slip faults, or by glide horizons of limited strike extent. Localized loading by a thickening and advancing thrust wedge would be expected to produce a corresponding arcuate depocentre in the foredeep, immediately adjacent to the salient. Lenticular depocentres located adjacent to regions of active thrust loading were also postulated by Catuneanu *et al.* (2000) based on observation of a laterally-migrating depocentre in the Campanian–Paleocene strata of Alberta. Major changes in fluvial paleocurrent directions noted in Permo-Triassic foredeep strata of the Karoo Basin were similarly interpreted to reflect episodic, along-strike tilting of the basin in response to the emplacement of localized thrust loads (Catuneanu and Elango 2001). In the latter case, pulses of thrust advance took place on an average timescale of 660 kyr.

Collectively, these observations imply that, at any given time, thrust sheets thicken and advance on fronts c. 100–300 km long, producing a corresponding arcuate pattern of subsidence in the western, proximal part of the foredeep. As stress is relieved, and the rate of thickening diminishes in one sector of the deformed belt, stress accumulates in an adjacent area, which then undergoes thickening until a new critical taper is achieved, driving isostatic subsidence in the adjacent foredeep. In consequence, the fill of the foredeep, if dissected in sufficient detail, comprises a series of overlapping, arcuate lenses of sediment. The studies noted above suggest that each cycle of active thrust-wedge thickening, followed by quiescence, and even erosion-related isostatic uplift, takes place on a timescale of c. 200–800 kyr.

Effect of deep-seated structural elements on the distal foredeep

In the eastern part of the foredeep, closer to the forebulge axis, well control is abundant and high-resolution subsurface correlation allows recognition of five master bounding surfaces that define five tectono-stratigraphic units that show short-wavelength (c. 100 km or less), thickening and thinning along roughly linear trends (Text-figs 9–13). Correlation of allomembers *within* each tectono-stratigraphic unit shows that allomembers have locally been *erosionally truncated*. The spatial pattern of erosion of strata is highly variable; in places erosion is nearly parallel to the forebulge but elsewhere is at a high angle (Text-figs 9–13). These patterns cannot be explained simply in terms of regional flexural subsidence driven by the load of the orogen.

The genesis of the discrete regions of erosion in the forebulge-proximal (eastern) part of the foredeep may, instead be related to the structure of the underlying Precambrian rocks. Aeromagnetic data, which reflect changes in the magnetic susceptibility of rocks in the upper part of the Precambrian basement, provide the primary basis for mapping the boundaries of the various geophysical anomaly domains beneath the Phanerozoic cover. Interpretation of basement structure is supplemented by Bouguer gravity data, although this signal is strongly overprinted by the effect of the thickness of the Phanerozoic sedimentary cover, which increases to the west (Villeneuve *et al.* 1993; Pilkington *et al.* 2000; Lyatsky *et al.* 2005; Ekpo *et al.* 2018). The Precambrian basement is interpreted to be a collage of terranes that were sutured together during development of Laurentia in the Archaean and Proterozoic (Hoffman 1988; Ross *et al.* 1991; Villeneuve *et al.* 1993; Pilkington *et al.* 2000).

Many stratigraphic investigations of the Cretaceous foreland basin in both Canada and the USA have concluded that the basin is partitioned into numerous blocks that have experienced differential vertical movement, postulated to have taken place on faults, some of which may extend down to the Precambrian basement (Anna 1986; Curry 1986; Merewether and Cobban 1986; Shurr and Rice 1986; Schwartz and DeCelles 1988; Edwards and Brown 1994; Edwards *et al.* 1995; Gay 2001; Lyatsky *et al.* 2005; Plint and Wadsworth 2006; Vakarelov *et al.* 2006; Vakarelov and Bhattacharya 2009; Grifi *et al.* 2013; Schultz *et al.* 2019). Despite the presence of many linear isopach

features and anomalous facies juxtapositions in the stratigraphic record, geophysical studies (Ross and Eaton 1999, 2001; Pană 2003; Lyatsky *et al.* 2005; Ekpo *et al.* 2018), have emphasized the difficulty of *proving* that these anomalies are directly related to faults in the Phanerozoic section, and/or that the postulated faults extend down into the Precambrian basement. Much of the difficulty in proving the existence of reactivated basement faults is due to the scarcity of public-domain seismic data, the lack of coherent reflections in the Precambrian rocks, and the weak magnetic and gravity signal generated by such faults.

Heller *et al.* (2003) considered mechanisms that could cause subtle topographic uplift and subsidence on a vertical scale of meters to tens of meters. Their modeling suggested that pre-existing basement faults were unlikely to be reactivated as a result of an increase in the in-plane stress level within the plate. On the other hand, models of the crust that included stronger and weaker zones, produced vertical deflections of c. 2–40 m over ≤100 km in response to an increase in in-plane stress.

Thus, both observations and modeling indicate that localized vertical movement can take place in response to changes in the stress level in the crust. Such movements may take place where discrete faults, or fault zones offset the Precambrian basement, or where stress is concentrated across zones where rock strength changes, such as the boundaries of Precambrian domains.

Precambrian basement and Coniacian sedimentation

In order to assess the possible influence of geophysical domain boundaries on the development of tectono-stratigraphic units A–E, the isopach maps for each unit were overlain on the corresponding portion of the aeromagnetic anomaly map (Text-fig. 15A–E). Within the study area, seven geophysical domains have been identified (Text-fig. 15F; Ross *et al.* 1991, 1995; Villeneuve *et al.* 1993; Eaton *et al.* 1995; Pilkington *et al.* 2000). However, comparison of the isopach patterns in the Coniacian cover to the distribution of domain boundaries in the Precambrian rocks some 1,800 to 2,200 m below reveals no obvious spatial correspondence (Text-fig. 15).

Edwards and Brown (1996) and Lyatsky *et al.* (2005) provide a number of maps showing many 'lineaments' interpreted from aeromagnetic data. These 'lineaments' were overlain on our isopach maps for units A–E. Despite the abundance of interpreted lineaments (which tended to have northwest-southeast trends), none showed any clear relationship to the patterns in our isopach maps. The mechanism(s) and structural elements that are suspected to have been responsible for the patterns of erosion in the mapped Coniacian strata cannot, therefore, be identified with any confidence.

Eustatic sea-level changes

Each tectono-stratigraphic unit, except unit A, comprises several component allomembers, each of which records a cycle of relative sea-level rise and fall, and which can be interpreted as a distal expression of a depositional sequence (Plint *et al.* 2017). Unit A comprises several upward-shoaling successions (or parasequences) but these are relatively subtle and were not designated as distinct allomembers (Plint *et al.* 2017; Hooper 2019). In the western outcrop belt, several allomembers have a pebble lag mantling the flooding surface. Most commonly, the pebbles are reworked phosphate or siderite clasts that provide no proof of subaerial emergence but do suggest submarine erosion and concentration of early diagenetic nodules. A few surfaces (e.g., CS1, CS4, Tmbk), however, carry extra-basinal chert pebbles indicative of subaerial emergence of the ramp and fluvial delivery of pebbles to a lowstand shoreline (Plint *et al.* 2017). In the subsurface study area however, limited core provides sparse evidence of extra-basinal pebble lags and hence the seaward extent of lowstand emergence, except on surface Tmbk, can not be established (Grifi *et al.* 2013; Text-figs 4–7).

All allomembers contain evidence for deposition above storm wave base in the form of wave and combined-flow ripples in very fine sand and coarse silt. This, coupled with the absence of clinoform stratal geometries, suggests that the sea floor formed a homoclinal ramp, shelving very gradually towards the north-east (Plint *et al.* 2017; Hooper 2019). Potentially, sediment would have accumulated to fill a 'mud accommodation envelope', above which sediment would be re-suspended by ambient wave energy and redistributed laterally to an area of greater accommodation (cf. Varban and Plint 2008; Plint *et al.* 2012b).

The fact that most allomembers show gradual depositional thinning towards the north-east is commensurate with long-term flexural subsidence, increasing towards the south-west (Text-fig. 8). The evidence for erosion and reworking of the top surface of allomembers implies either complete cessation of sediment supply, accompanied by reworking by basinal processes, or, more probably, some degree of relative sea-level fall and accommodation loss, lead-

ing to submarine erosion. Given that 24 allomembers are recognized in the Muskiki and Marshybank members, an average allomember duration (3 myr/24) of c. 125 kyr may be calculated. It seems unlikely that tectonic uplift *and* subsidence of the foredeep took place on such a short timescale and it is therefore concluded that high-frequency eustatic oscillations modulated the long-term accommodation generated by flexural subsidence (Plint 1991; Plint *et al.* 2107, 2022).

Evidence in support of an eustatic mechanism is also provided by physical and faunal evidence. Plint *et al.* (2022) showed that *Cremnoceramus crassus* (Petrascheck, 1903) occurred immediately above a major flooding surface in both Alberta and the Czech Republic, indicative of an eustatic control on the transgression. Allomembers CA2–CA4, mapped through the central Alberta Foothills, contain *Inoceramus gibbosus* Schlüter, 1877, which defines the uppermost zone of the Lower Coniacian (Plint *et al.* 2017; Walaszczyk *et al.* 2017). This species is known from a few localities in Europe but otherwise is absent in that region, nor has it been recorded in sections in the western United States. The top of the *I. gibbosus* Zone is defined by surface CS4, which has a veneer of extra-basinal clasts, indicative of subaerial emergence. Walaszczyk *et al.* (2017) inferred that the *I. gibbosus* Zone is preserved in the western Alberta foredeep as a result of rapid tectonic subsidence, whereas its absence from most shelf regions in Europe and North America is due to an eustatic fall that left those areas emergent, or too shallow to accumulate sediment.

DEPOSITIONAL HISTORY

The history of deposition, deformation, and erosion is here deduced from the geometry and internal stratal organization of tectono-stratigraphic units A–E, and their component allomembers. Text-fig. 16 is drawn to scale and is an attempt to summarize the sequence of events seen in the east-west (dip-oblique) view based on the log cross-sections in Townships 28 (Text-fig. 4) and 42 (Text-fig. 5). Similarly, Text-fig. 17 represents the stratigraphy seen in the north-south (strike-oblique) log cross-sections in Ranges 28 (Text-fig. 6) and 16 (Text-fig. 7). Text-figs 16 and 17 interpret 'background' deposition to have taken place on a planar, near-horizontal sea floor across which muddy sediment was efficiently redistributed, mainly by storm-generated combined flows. Accommodation was modulated by modest eustatic changes on a Milankovitch timescale. Regional (300–400 km) differential flexural subsidence resulted in each allomember thickening very gradually to the south-west. This mode of sedimentation was episodically punctuated by episodes of differential erosion on a horizontal scale of c. 50–100 km. The plan-view shape, scale and orientation of the eroded segments of stratigraphy shown in Text-figs 9–13, is too complex and localized to be explicable in terms of regional flexural effects, such as uplift or subsidence of the forebulge.

One may postulate that the sea floor was eroded into broad troughs, leaving remnant upstanding areas. However, this is difficult to envisage in terms of process (rivers, submarine currents?), and is not supported by the stratal geometry: if topographically low troughs had been eroded out, the subsequent fill would thin laterally towards, and onlap, the margins of the trough. This stratal architecture is not seen.

An alternative possibility is that the sea floor was deformed into a series of arches and troughs of c. 10 to 20 m amplitude, across ?basement controlled 'hinge zones'. Allomembers show little or no thinning towards the thinner parts, nor thickening towards the thicker parts of the tectono-stratigraphic units. In other words, at the time they were being deposited, the allomembers did not 'feel' subsidence or uplift across localized 'hinge zones'. It must therefore be inferred that the development of arches and troughs was an episodic, and relatively rapid process that punctuated tectonically quiescent 'background' sedimentation. Arches underwent erosion, presumably submarine, in response to uplift and accommodation loss, whereas strata were preferentially preserved in troughs. Beveling surfaces are also flooding surfaces and therefore probably record both eustatic fall and subsequent rise. Eustatic fall would have enhanced submarine erosion of arches, and also reduced accommodation across the entire ramp, promoting the long-distance reworking and advection of both eroded and newly-delivered sediment, forming an erosional or by-pass surface. There is no evidence (e.g., onlap onto the flanks of troughs), that sediment eroded from the arches accumulated in adjacent troughs: the surplus material appears to have been completely exported from the study area.

Subsequent eustatic rise, coupled with long-term regional subsidence would have provided accommodation for the next package of allomembers, deposited under relatively quiescent 'background' conditions. It is not possible to quantify the time represented by each tectono-eustatic package of rock, nor the time missing at the beveling surfaces. Intuitively, it would seem likely that most of the 600 kyr average span of each unit is represented by sediment, with a relatively

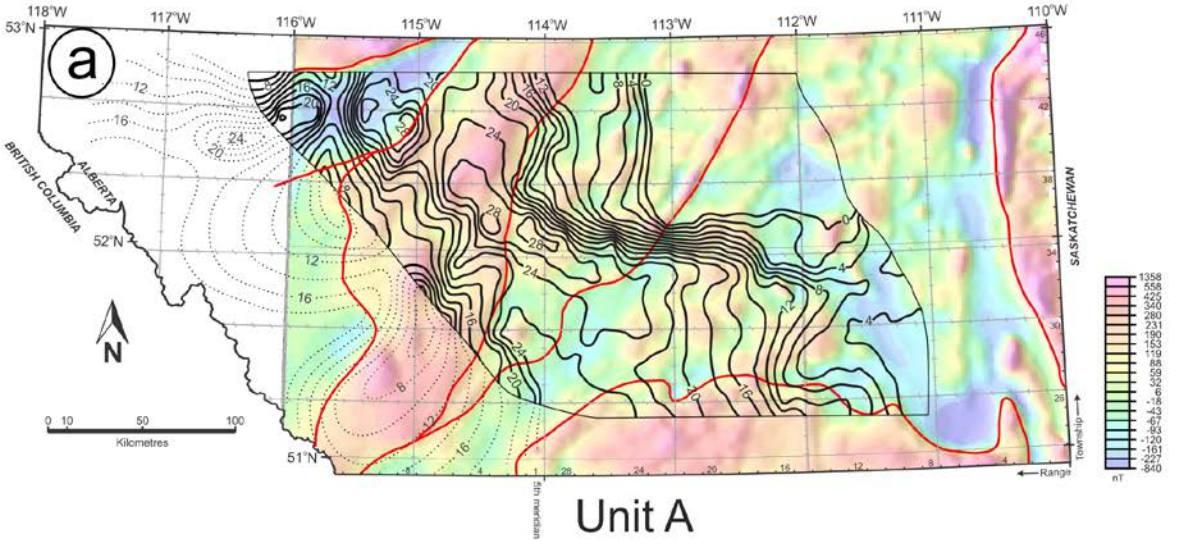
a
118°W
117°W
116°W
115°W
114°W
113°W
112°W
111°W
110°W
53°N
52°N
51°N
BRITISH COLUMBIA
ALBERTA
SASKATCHEWAN
N
0 10 50 100
Kilometres
Township
Range
4th meridian
nT
Unit A

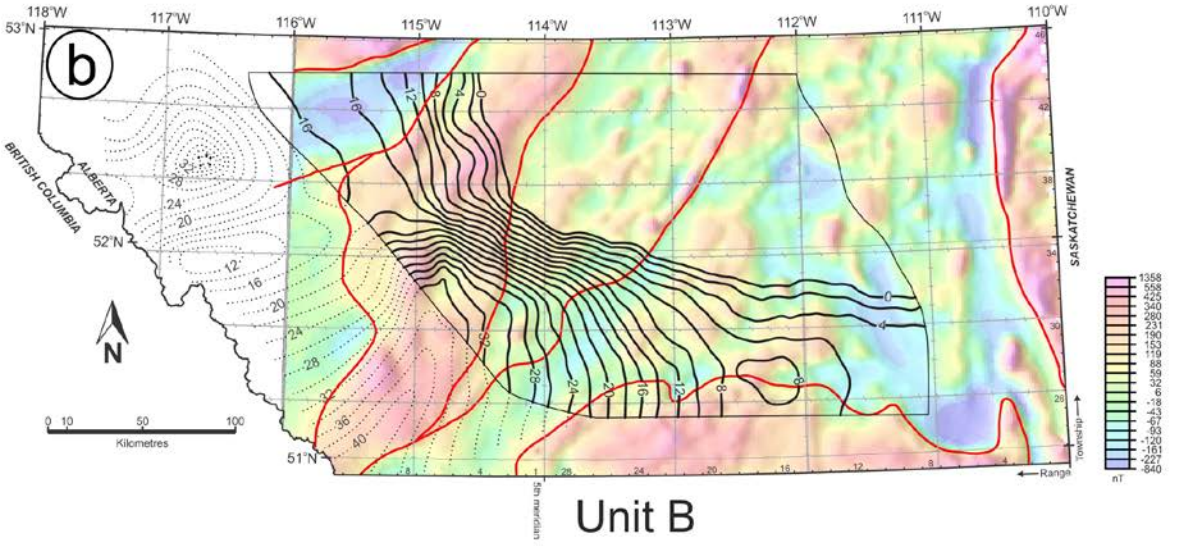
b
118°W
117°W
116°W
115°W
114°W
113°W
112°W
111°W
110°W
53°N
52°N
51°N
BRITISH COLUMBIA
ALBERTA
SASKATCHEWAN
N
0 10 50 100
Kilometres
Township
Range
4th meridian
nT
Unit B

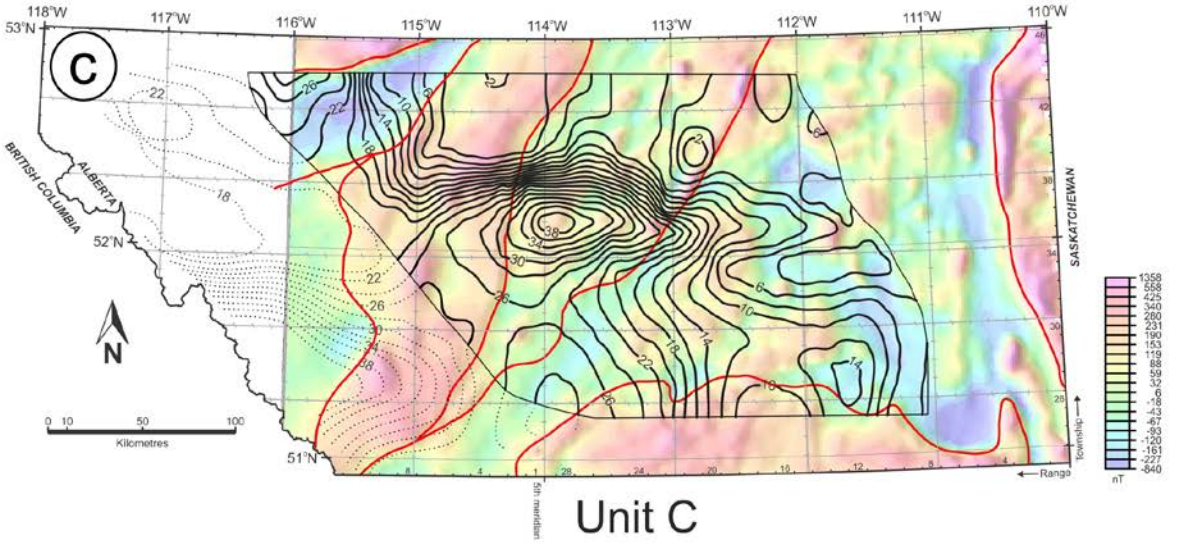
c
118°W
117°W
116°W
115°W
114°W
113°W
112°W
111°W
110°W
53°N
52°N
51°N
BRITISH COLUMBIA
ALBERTA
SASKATCHEWAN
N
0 10 50 100
Kilometres
Township
Range
4th meridian
nT
Unit C

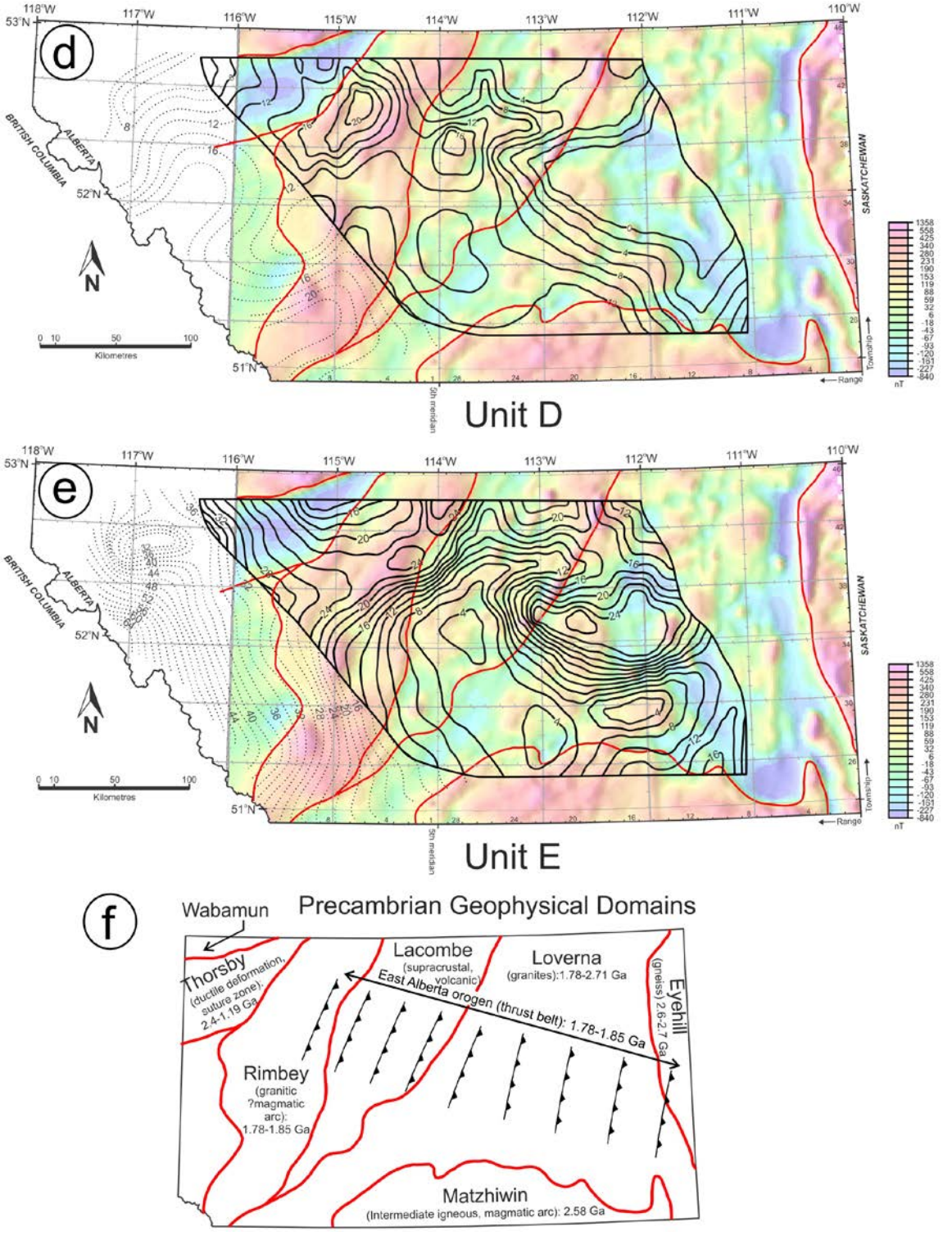

← Text-fig. 15. Panels A–E show the aeromagnetic map of the study area with, superimposed, isopach maps of the five tectono-stratigraphic units A to E. The boundaries of Precambrian geophysical domains are shown in red. F – Summary of the age, structure and rock type of the various geophysical domains. The Thorsby domain is interpreted as a major zone of ductile deformation between the Hearne and Rae terranes, and continues to the NE as the Snowbird Tectonic Zone. Aeromagnetic map courtesy of Mark Pilkington; geophysical domain data compiled from Ross *et al.* (1991, 1995), Eaton *et al.* (1995) and Hope *et al.* (1999). There is no obvious correspondence of any of the Coniacian troughs and arches to the boundaries of the geophysical domains in the Precambrian basement.

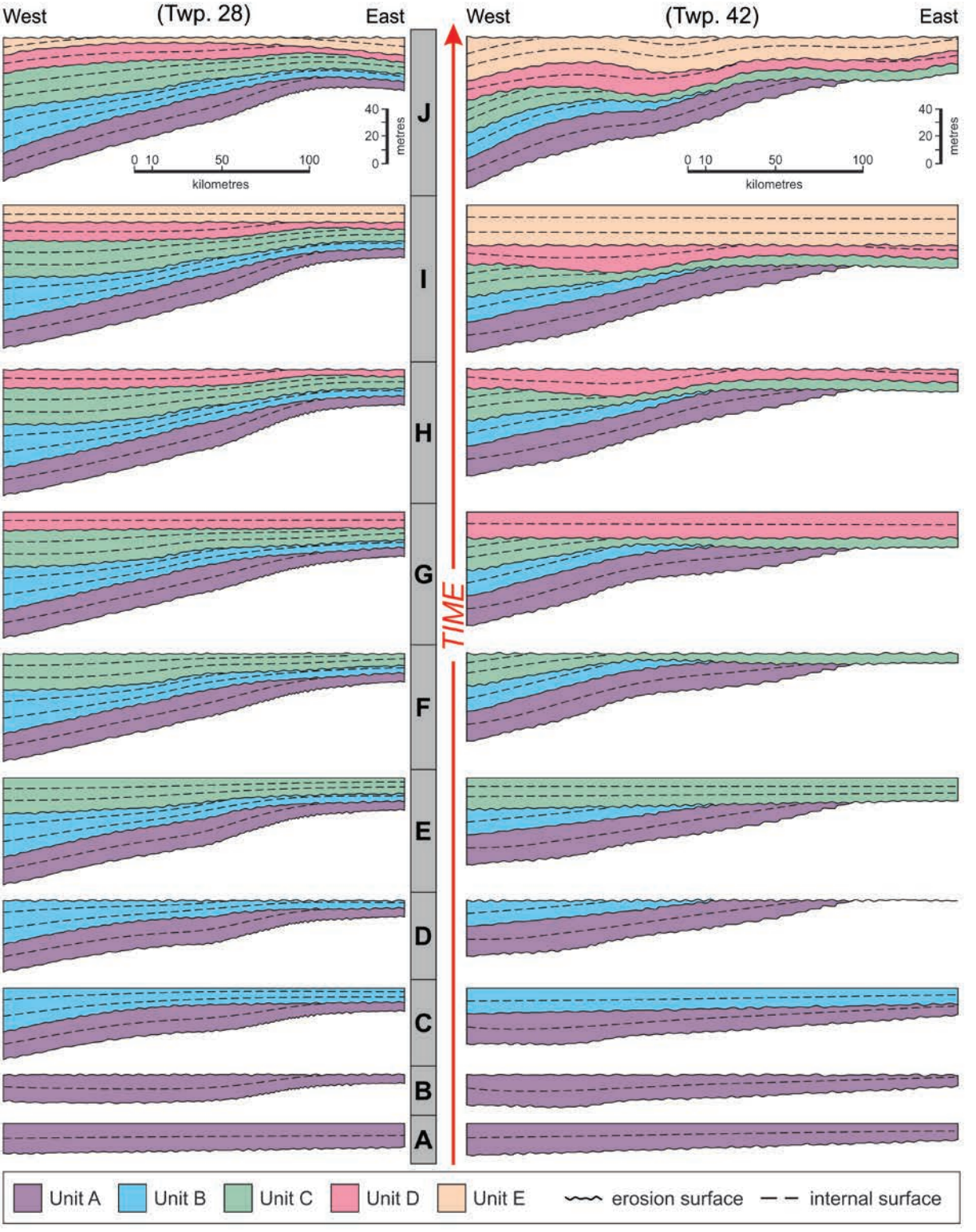

Text-fig. 16. Summary of depositional history (to scale) in dip-oblique view. The gradual westward thickening of allomembers reflects long-term flexural subsidence. It is inferred that deposition of units A–E took place when genesis of arches and troughs was inactive. The thinning and disappearance of any given unit is almost entirely due to erosional truncation over the crests of arches. The cycle of: a) 'background' deposition of muddy sediment; b) formation of arches and troughs, followed by c) erosional planation was repeated for each of the five units A through E.

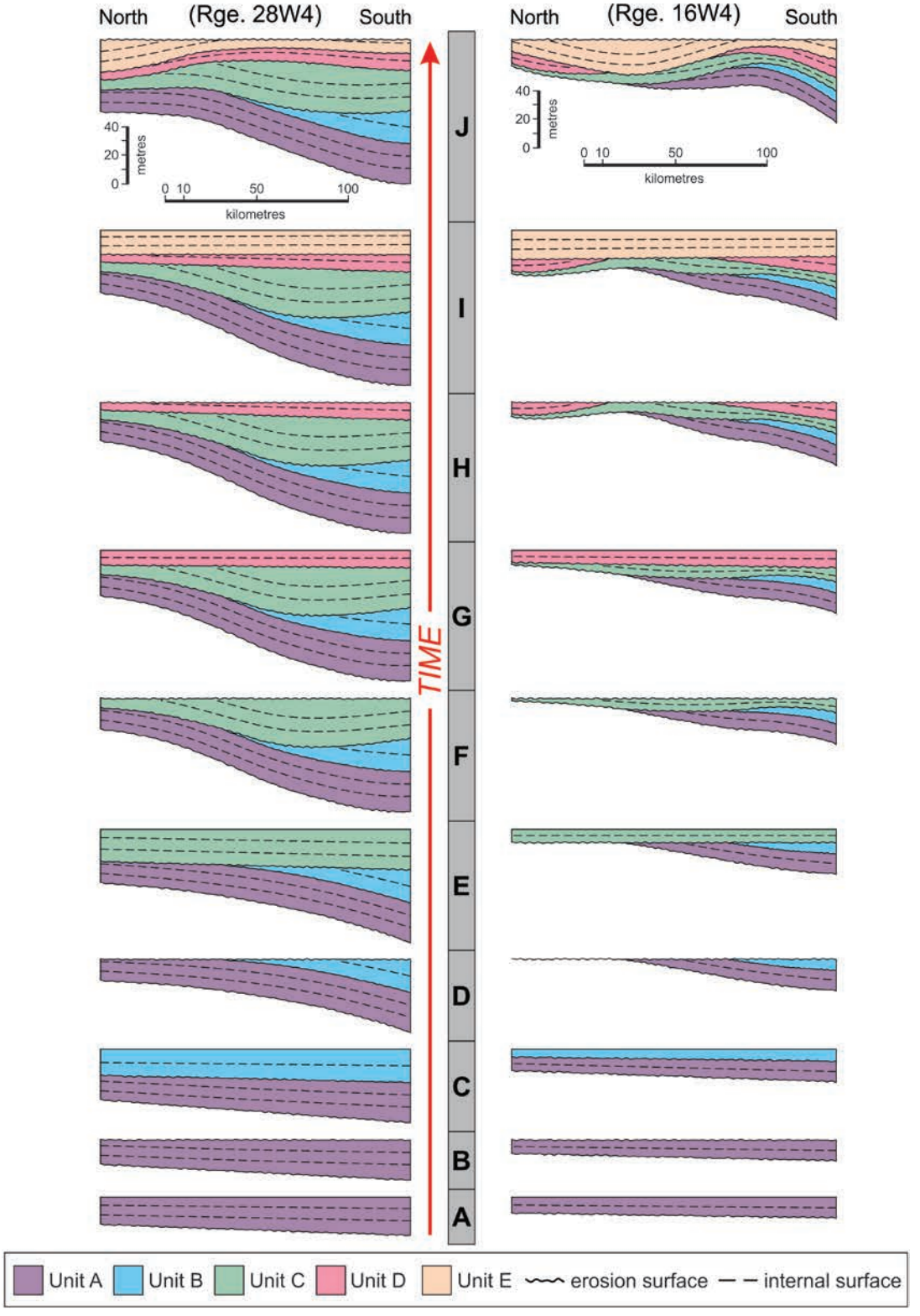

Text-fig. 17. Summary of depositional history in strike-oblique view, showing the development of arches, with attendant erosional truncation, and intervening troughs. The pronounced thickening towards the south is mainly a reflection of the trend of the section, oblique to the foredeep. As in the dip-oblique view, the three-part cycle involved deposition on a planar sea floor, followed by deformation and then erosional beveling, followed by the next cycle with deposition on a tectonically-inactive sea floor.

short time recorded by the differential vertical movement of 'basement blocks' and formation of beveling surfaces.

Although it has not been possible to identify any specific underlying Precambrian tectonic elements (e.g., faults, forced folds, crustal weak zones) that could have been responsible for the observed changes in accommodation, it is assumed that some structural elements were episodically reactivated. Successive isopach maps show a certain reciprocal quality to vertical movements: an earlier arch was likely to become a trough during the next phase of deformation (compare units C, D and E in Text-fig. 14).

Because none of the features mapped in the Coniacian rocks can be related to underlying features in the Paleozoic succession, such as the trends of reef margins, differential compaction does not seem to have been a control on accommodation or erosion. Based on both stratigraphically constrained and modeling studies, it is here inferred that the temporally-discrete episodes of vertical uplift and subsidence were triggered by changes in stress regime within the crust (Heller *et al.* 1993).

The most closely comparable studies to that presented here are by Schultz *et al.* (2019) and Percy (2019). Schultz *et al.* (2019) investigated the stratigraphy of the Late Albian Joli Fou and Viking formations in a region adjacent to the northern limit of the present study area (approx. between Townships 45 and 66). Schultz *et al.* (2019) observed that one depositional sequence within the Viking Formation underwent marked thickening over a limited area; thickening was explained as a result of a short-lived episode of differential, syn-depositional subsidence. The isopach map presented in support of this interpretation (Schultz *et al.* 2019, their fig. 8) shows a lobe-like pattern of stratal thickening that the authors interpret to reflect differential subsidence over a region they term the 'Snowbird Anomaly Zone' (portrayed on other aeromagnetic maps as the Thorsby Low and Wabamun High, e.g., Ross *et al.* 1995). However, the isopach trends shown by Schultz *et al.* (2019, fig. 8) show only a vague correspondence to the margins of the 'Snowbird Anomaly Zone' (i.e., the northern boundary of the Wabamun domain and the southern boundary of the Thorsby domain), and isolines in the Viking strata trend across the domain boundaries with little or no deflection. Thus, although there is undoubted thickening within one sequence of the Viking Formation, the correspondence claimed by Schultz *et al.* (2019) between the pattern of thickening and the underlying aeromagnetic domain boundaries appears to be weak at best.

Percy (2019) studied mudstone-dominated strata of Late Cenomanian to Early Turonian age over c. 60,000 km^2 of south-western Alberta using c. 2000 wells. Facies distributions and isopach patterns were mapped for five allostratigraphically-defined units. Although in a few instances, facies distributions or isopach patterns showed a vague correspondence to Precambrian domain boundaries, there is little definitive evidence that 'basement lineaments' identified in public-domain data had any influence on patterns of sedimentation or erosion during Late Cenomanian to Early Turonian time. Inspection of the data presented in Percy (2019, chapter 5), suggests that regional flexural subsidence, linked to loading in the Cordillera appears to have been the dominant control on increased accommodation in the foredeep, and erosional beveling over the forebulge.

It seems safe to conclude that the patterns of uplift and subsidence mapped in Upper Albian, Upper Cenomanian to Lower Turonian, and Coniacian strata are comparable in that they *do not follow* aero-magnetically-defined basement structures.

Despite the complex history of deposition and erosion recorded by the Coniacian mudstones, the *net pattern of sediment accumulation*, defined by surfaces E7 and Tmbk, is a smoothly-thickening wedge of mudstone that *appears* to record continuous accumulation during steady flexural subsidence (Text-fig. 8). On a 2-D seismic section, it is possible that just the top and base of the studied succession will generate reflections that would appear to be near-parallel (cf. Hope *et al.* 1999), and the complex depositional history, revealed by high-resolution allostratigraphic correlation of well logs, would be undetectable. Although it is quite possible that 3-D seismic data might reveal structural features that controlled the pattern of arches and troughs, such data are not generally available to academic investigations. This realization may temper the interpretation of Hope *et al.* (1999), who concluded, on the basis of 2-D seismic profiles, that there is no evidence for reactivation of basement structures in the mudstone-dominated Cretaceous cover.

CONCLUSIONS

1. Shallow-marine, mudstone-dominated strata of the Coniacian Muskiki and Marshybank members are c. 100 m thick and were mapped over c. 45,000 km^2 of the foredeep region of the Western Canada Foreland Basin. In the study area described herein, 18 allomembers, typically c. 10 m thick, bounded by marine flooding surfaces or composite unconformi-

ties/flooding surfaces, were mapped. Allomembers thin very gradually towards the north-east (i.e., towards the forebulge).

2. The succession of 18 allomembers is partitioned into five 'tectono-stratigraphic units' A through E, by low-angle beveling unconformities that cut out c. 10 to 20 m of strata at unit boundaries. Each unit is inferred to have an average duration of c. 600 kyr. Strata in each unit are interpreted to have been deformed into arches and troughs on a length scale of 50–100 km. Strata were bevelled off over the crest of arches and were preserved in troughs. Allomember boundaries do not converge towards arches, nor diverge into troughs, implying that deformation of the basin floor did not occur syn-depositionally. Instead, deposition of a succession of allomembers took place on a low-gradient ramp subject only to subtle regional flexural subsidence, with accommodation modulated by Milankovitch-scale eustatic cycles. This 'background' style of deposition was episodically punctuated by a phase of vertical deformation. Strata elevated on arches were bevelled off, probably by submarine erosion that was amplified by minor eustatic fall. Erosion and lateral export of sediment produced a near-planar sea floor that, following the next eustatic rise, accumulated a new package of strata under tectonically quiescent conditions. That package in turn was warped and bevelled during the next phase of deformation.

3. Spanning c. 3 myr, the Coniacian strata, isopached collectively, show a very steady south-westward thickening into the foredeep. The crest of the forebulge lies c. 400 km north-east of the inferred Late Coniacian deformation front. This simple pattern contrasts markedly with isopach maps of the individual tectono-stratigraphic units, each of which reveals a complex pattern of uplift and subsidence across the eastern, more distal part of the foredeep. Tectono-stratigraphic units A and B are erosionally removed in an approximately rectangular area in the north-eastern part of the study area. Units C, D and E show discrete regions that underwent alternate uplift and subsidence, with arches becoming troughs, and vice versa. As a result of this 'compensation' style of deformation, *net* sediment accumulation through the Coniacian appears remarkably uniform.

4. Although the Precambrian basement beneath the study area is a complex collage of accreted terranes, no spatial correspondence can be demonstrated between terrane boundaries and the pattern of erosion mapped in the Coniacian cover rocks some 2 km above. Although surface deformation due to fault reactivation or deformation across 'weak zones' in the basement presents an attractive hypothetical possibility, this study has been unable to demonstrate a genetic, basement-cover relationship. The genetic mechanism responsible for the episodic pulses of localized differential uplift and subsidence therefore remains unexplained, although changes in in-plane stress are an appealing possibility.

5. The subtle, mud-on-mud unconformities that bound the five tectono-stratigraphic units in the mid- to distal part of the foredeep probably represent at least tens of thousands of years, but may be very difficult to recognize in core and are certainly undetectable in individual well logs. Furthermore, the spatially-complex removal of intervals of rock over ephemeral tectonic arches would render the succession of fossils incomplete, and potentially difficult to explain. This package of offshore mudstone can justifiably be compared to Emmental Cheese in being 'full of holes'!

Acknowledgements

This study builds on many years of investigation of Upper Cretaceous strata in Western Canada, that have been supported by numerous cycles of Discovery Grant funding provided to AGP by the Natural Sciences and Engineering Research Council of Canada. This long-term support is gratefully acknowledged. Additional funding was provided by Imperial Oil Ltd. and Husky Energy Ltd. EAH thanks the SEPM Foundation for a Student Assistance Grant to support her fieldwork. We are grateful to Divestco Ltd. (Calgary) who provided charge-free access to the digital well logs, and Imperial Oil for their donation of their microfiche log library. We also thank Pan Canadian Petroleum (now Cenovus Ltd.) for their donation of a gamma ray spectrometer which greatly facilitated outcrop to subsurface correlation. Cheerful field assistance was provided by Omar Al-Mufti, Piotr Angiel, Sarah CoDyre, Meriem Grifi, Stephen Morrow, Tessa Plint and Kathleen Vannelli, while Ireneusz Walaszczyk worked tirelessly alongside us to collect molluscan fossils. We thank Alina Shchepetkina and Bruce Hart for informal reviews of the manuscript, and Journal Referees Jessica Flynn and, in particular Zhiyang Li, for their very constructive comments that prompted significant revision and clarification of the manuscript.

REFERENCES

Anna, L.O. 1986. Structural influences on Cretaceous sedimentation, northern Great Plains. In: Peterson, J.A. (Ed.), Paleotectonics and sedimentation in the Rocky Mountain Region, United States. *American Association of Petroleum Geologists, Memoir*, **41**, 173–191.

Beaumont, C., Quinlan, G.M. and Stockmal, G.S. 1993. The evolution of the Western Interior Basin: Causes, consequences and unsolved problems. In: Caldwell, W.G.E. and Kauffman, E.G. (Eds), Evolution of the Western Interior Basin. *Geological Association of Canada, Special Paper*, **39**, 97–117.

Benyon, C., Leier, A., Leckie, D.A., Webb, A., Hubbard, S.M. and Gehrels, G.E. 2014. Provenance of the Cretaceous Athabasca oil sands, Canada: Implications for continent-scale sediment transport. *Journal of Sedimentary Research*, **84**, 136–143.

Blum, M. and Pecha, M. 2014. Mid-Cretaceous to Paleocene North American drainage reorganization from detrital zircons. *Geology*, **42**, 607–610.

Buckley, R.A., Plint, A.G., Henderson, O.A., Krawetz, J.R. and Vannelli, K.M. 2016. Ramp sedimentation across a middle Albian, Arctic embayment: Influence of subsidence, eustasy and sediment supply on stratal architecture and facies distribution, Lower Cretaceous, Western Canada Foreland Basin. *Sedimentology*, **63**, 699–742.

Catuneanu, O. and Elango, H.N. 2001. Tectonic control on fluvial styles: the Balfour Formation of the Karoo Basin, South Africa. *Sedimentary Geology*, **140**, 291–313.

Catuneanu, O., Sweet, A.R. and Miall, A.D. 2000. Reciprocal stratigraphy of the Campanian–Paleocene Western Interior of North America. *Sedimentary Geology*, **134**, 235–255.

Cobban, W.A., Erdmann, C.E., Lemke, R.W. and Maughan, E.K. 1976. Type sections and stratigraphy of the members of the Blackleaf and Marias River formations (Cretaceous) of the Sweetgrass Arch, Montana. *United States Geological Survey Professional Paper*, **974**, 63 pp.

Curry, W.H. 1986. Subtle middle Cretaceous paleotectonic deformation of Frontier and Lower Cody rocks in Wyoming. In: Peterson, J.A. (Ed.), Paleotectonics and sedimentation in the Rocky Mountain Region, United States. *American Association of Petroleum Geologists, Memoir*, **41**, 469–479.

Dahlstrom, C.D.A. 1969. Balanced cross sections. *Canadian Journal of Earth Sciences*, **6**, 743–757.

Donaldson, W.S., Plint, A.G. and Longstaffe, F.J. 1998. Basement tectonic control on distribution of shallow marine Bad Heart Formation: Peace River Arch area, NW Alberta. *Bulletin of Canadian Petroleum Geology*, **46**, 576–598.

Donaldson, W.S., Plint, A.G. and Longstaffe, F.J. 1999. Tectonic and eustatic control on deposition and preservation of Cretaceous ooidal ironstone and associated facies: Peace River Arch area, NW Alberta, Canada. *Sedimentology*, **46**, 1159–1182.

Eaton, D.W., Milkereit, B., Ross, G.M., Kanasewich, E.R., Geis, W., Edwards, D.J., Kelsch, L. and Varsek, J. 1995. Lithoprobe basin-scale seismic profiling in central Alberta: influence of basement on the sedimentary cover. *Bulletin of Canadian Petroleum Geology*, **43**, 65–77.

Edwards, D.J. and Brown, R.J. 1994. Tectonic heredity in west-central Alberta: recognition and significance. In: Ross, G.R. (Ed.), Lithoprobe Alberta basement transects, Report of Transect Workshop, February 14–15, 1994, Calgary, AB, Lithoprobe Report 37, 164–194. Lithoprobe Secretariat, University of British Columbia; Vancouver B.C.

Edwards, D.J. and Brown, R.J. 1996. A geophysical perspective on the question of basement involvement with the distribution of Upper Devonian carbonates in central Alberta. In: Ross, G.M. (Ed.), Lithoprobe Alberta basement transects, Report of Transect Workshop, February 29 and March 1, 1996, Calgary, Lithoprobe Report 51, 133–197. Lithoprobe Secretariat, University of British Columbia; Vancouver B.C.

Edwards, D.J., Lyatsky, H.V. and Brown, R.J. 1995. Basement fault control on Phanerozoic stratigraphy in the Western Canada sedimentary Province: Integration of potential field and lithostratigraphic data. In: Ross, G.M. (Ed.), Lithoprobe Alberta basement transects, Report of Transect Workshop, April 10–11, 1995, Calgary, Lithoprobe Report 47, 181–224. Lithoprobe Secretariat, University of British Columbia; Vancouver B.C.

Ekpo, E., Eaton, D. and Weir, R. 2018. Basement tectonics and fault reactivation in Alberta based on seismic and potential field data. In: Okiwelu, A. (Ed.), Geophysics. IntechOpen, 65–80. http://dx.doi.org/10.5772/intechopen.72766

Evenchick, C.A., McMechan, M.E., McNichol, V.J. and Carr, S.D. 2007. A synthesis of the Jurassic–Cretaceous tectonic evolution of the central and southeastern Canadian Cordillera: Exploring links across the orogen. In: Sears, J.W., Harms, T.A. and Evenchick, C.A. (Eds), Whence the mountains? Inquiries into the evolution of orogenic systems: A volume in honor of Raymond A. Price. *Geological Society of America, Special Paper*, **433**, 117–145.

Gay, S.P. 2001. Comment on: Basement reactivation in the Alberta Basin: Observational constraints and mechanical rationale. *Bulletin of Canadian Petroleum Geology*, **49**, 426–428.

Grifi, M.D. 2012. Stratigraphy and sedimentology of the Late Cretaceous (Coniacian) Muskiki and Marshybank members, southern Alberta and northwestern Montana, 216 pp. Unpublished M.Sc. thesis, University of Western Ontario; London, Canada.

Grifi, M.D., Plint, A.G. and Walaszczyk, I. 2013. Rapidly changing styles of subsidence revealed by high-resolution mudstone allostratigraphy: Coniacian of Sweetgrass Arch area, southern Alberta and northern Montana. *Canadian Journal of Earth Sciences*, **50**, 439–461.

Heller, P.L., Breekman, F., Angevine, C.L., and Cloetingh, S.A.P.L. 1993. Cause of tectonic reactivation and subtle uplifts in the Rocky Mountain region and its effect on the stratigraphic record. *Geology*, **21**, 1003–1006.

Hoffman, P.F. 1988. United plates of America, the birth of a craton: Early Proterozoic assembly and growth of Laurentia. *Annual Review of Earth and Planetary Sciences*, **16**, 543–603.

Hooper, E.A. 2019. Allostratigraphy and sedimentology of the Muskiki and Marshybank members of the Wapiabi Formation (Upper Cretaceous, Coniacian) in southwestern Alberta, Canada, 217 pp. Unpublished Ph.D. thesis, University of Western Ontario; London, Canada.

Hope, J., Eaton, D.W. and Ross, G.M. 1999. Lithoprobe seismic transect of the Alberta Basin: Compilation and review. *Bulletin of Canadian Petroleum Geology*, **47**, 331–345.

Hu, Y.G. and Plint, A.G. 2009. An allostratigraphic correlation of a mudstone-dominated syn-tectonic wedge: The Puskwaskau Formation (Santonian–Campanian) in outcrop and subsurface, Western Canada foreland basin. *Bulletin of Canadian Petroleum Geology*, **57**, 1–33.

Jordan, T.E. and Flemings, P.F. 1991. Large-scale stratigraphic architecture, eustatic variation, and unsteady tectonism: A theoretical evaluation. *Journal of Geophysical Research*, **96B4**, 6681–6699.

Kauffman, E.G. 1977. Geological and biological overview: Western Interior Cretaceous Basin: *The Mountain Geologist*, **14**, 75–99.

Landman, N.H., Plint, A.G. and Walaszczyk, I. 2017. Scaphitid ammonites from the Upper Cretaceous (Coniacian–Santonian) Western Canada Foreland Basin. *Bulletin of the American Museum of Natural History*, **414**, 104–172.

Leckie, D.A. and Cheel, R.J. 1997. Sedimentology and depositional history of Lower Cretaceous coarse-grained clastics, southwest Alberta and southeast British Columbia. *Bulletin of Canadian Petroleum Geology*, **45**, 1–24.

Leier, A.L. and Gehrels, G.E. 2011. Continental-scale detrital zircon provenance signatures in Lower Cretaceous strata, western North America. *Geology*, **39**, 399–402.

Li, Z. and Aschoff, J. 2022. Constraining the effect of dynamic topography on the development of Late Cretaceous Cordilleran foreland basin, western United States. *Geological Society of America, Bulletin*, **134**, 446–462.

Li, Z. and Schieber, J. 2022. Correlative conformity or subtle unconformity? The distal expression of a sequence boundary in the Upper Cretaceous Mancos Shale, Henry Mountains Region, Utah, U.S.A: *Journal of Sedimentary Research*, **92**, 635–657.

Liu, S., Nummedal, D. and Gurnis, M. 2014. Dynamic versus flexural controls of Late Cretaceous Western Interior Basin, USA. *Earth and Planetary Science Letters*, **389**, 221–229.

Lyatsky, H.V., Pană, D.I. and Grobe, M. 2005. Basement structure in central and southern Alberta: Insights from gravity and magnetic maps. *Alberta Geological Survey Special Report*, **72**, 76 pp.

Macedo, J. and Marshak, S. 1999. Controls on the geometry of fold-thrust belts. *Geological Society of America, Bulletin*, **111**, 1808–1822.

Macquaker, J.S.H., Taylor, K.G. and Gawthorpe, R.L. 2007. High-resolution facies analysis of mudstones: Implications for paleoenvironmental and sequence stratigraphic interpretations of offshore ancient mud-dominated successions. *Journal of Sedimentary Research*, **77**, 324–339.

Mars, J.C. and Thomas, W.A. 1999. Sequential filling of a foreland basin. *Journal of Sedimentary Research*, **69**, 1191–1208.

Marshak, S., Wilkerson, M.S. and Hsui, A.T. 1992. Generation of curved fold-thrust belts: Insight from simple physical and analytical models. In: Clay, K.R. (Ed.), Thrust Tectonics, 83–92. Chapman and Hall; London.

McMechan, M.E. and Thompson, R.I. 1993. The Canadian Cordilleran fold and thrust belt south of 66ºN and its influence on the Western Interior Basin. In: Caldwell, W.G.E. and Kauffman, E.G. (Eds), Evolution of the Western Interior Basin. *Geological Association of Canada, Special Paper*, **39**, 73–90.

McNeil, D.H. 1984. The eastern facies of the Cretaceous System in the Canadian Western Interior. In: Stott, D.F. and Glass, D.J. (Eds), The Mesozoic of middle North America. *Canadian Society of Petroleum Geologists, Memoir*, **9**, 145–171.

Merewether, E.A. and Cobban, W.A. 1986. Biostratigraphic units and tectonism in the mid-Cretaceous foreland of Wyoming, Colorado, and adjoining areas. In: Peterson, J.A. (Ed.), Paleotectonics and sedimentation in the Rocky Mountain Region, United States. *American Association of Petroleum Geologists, Memoir*, **41**, 443–468.

Miall, A.D. and Catuneanu, O. 2019. The Western Interior Basin. In: Miall, A.D. (Ed.), The sedimentary basins of the United States and Canada (2nd Ed.), 401–443. Elsevier; Amsterdam.

Mitrovica, J.X., Beaumont, C. and Jarvis, G.T. 1989. Tilting of continental interiors by the dynamical effects of subduction. *Tectonics*, **8**, 1079–1094.

North American Commission on Stratigraphic Nomenclature. 2005. North American Stratigraphic Code. *American Association of Petroleum Geologists, Bulletin*, **89**, 1547–1591.

Nielsen, K.S., Schröder-Adams, C.J., and Leckie, D.A. 2003. A new stratigraphic framework for the Upper Colorado Group (Cretaceous) in southern Alberta and southwestern Saskatchewan, Canada. *Bulletin of Canadian Petroleum Geology*, **51**, 304–346.

Nielsen, K.S., Schröder-Adams, C.J., Leckie, D.A., Haggart, J.W. and Elberdak, K. 2008. Turonian to Santonian paleoenvironmental changes in the Cretaceous Western Interior Sea: The Carlisle and Niobrara formations in southern Alberta and southwestern Saskatchewan, Canada. *Palaeogeography, Palaeoclimatology, Palaeoecology*, **270**, 64–91.

Pană, D.I. 2003. Precambrian basement of the Western Canada Sedimentary Basin in northern Alberta, 39 pp. Alberta Geological Survey, Earth Sciences Report 2002-02; Edmonton, Alberta.

Percy, E.L. 2019. Depositional processes and characterization of multi-scale heterogeneity of an organic-rich mudstone, Second White Specks Formation, SW Alberta. Unpub-

lished Ph.D. thesis, 207 pp. University of Calgary; Calgary, Canada.

Petrascheck, W. 1903. Ueber Inoceramen aus der Kreide Böhmens und Sachsen. *Jahresberichte der Kaiserlisch-Königlichen Geologischen Reichsanstalt*, **53** (1), 153–168.

Pilkington, M., Miles, W.F., Ross, G.M., and Roest, W.R. 2000. Potential-field signatures of buried Precambrian basement in the Western Canada Sedimentary Basin. *Canadian Journal of Earth Sciences*, **37**, 1453–1471.

Plint, A.G. 1990. An allostratigraphic correlation of the Muskiki and Marshybank formations (Coniacian–Santonian) in the Foothills and subsurface of the Alberta Basin. *Bulletin of Canadian Petroleum Geology*, **38**, 288–306.

Plint, A.G. 1991. High-frequency relative sea level oscillations in Upper Cretaceous shelf clastics of the Alberta Foreland Basin: Evidence for a Milankovitch-scale glacio-eustatic control? In: Macdonald, D.I.M. (Ed.), Sedimentation, Tectonics and Eustacy. *International Association of Sedimentologists, Special Publication*, **12**, 409–428.

Plint, A.G., Hooper, E.A., Grifi, M.D., Walaszczyk, I., Landman, N.H., Gröcke, D.R., Trabucho Alexandre, J.P. and Jarvis, I. 2017. Integrated, high-resolution allostratigraphic, biostratigraphic and carbon-isotope correlation of Coniacian strata (Upper Cretaceous), western Alberta and northern Montana. *Bulletin of the American Museum of Natural History*, **414**, 9–52.

Plint, A.G., Krawetz, J.R., Buckley, R.A., Vannelli, K.M. and Walaszczyk, I. 2018. Tectonic, eustatic and climatic controls on marginal marine sedimentation across a flexural depocentre: Paddy Member of Peace River Formation (Late Albian), Western Canada Foreland Basin. *The Depositional Record*, **4**, 4–58.

Plint, A.G., Macquaker, J.H.S. and Varban, B.L. 2012b. Shallow-water, storm-influenced sedimentation on a distal, muddy ramp: Upper Cretaceous Kaskapau Formation, Western Canada foreland basin. *Journal of Sedimentary Research*, **82**, 801–822.

Plint, A.G. and Norris, B. 1991. Anatomy of a ramp margin sequence: Facies successions, paleogeography and sediment dispersal patterns in the Muskiki and Marshybank formations, Alberta Foreland Basin. *Bulletin of Canadian Petroleum Geology*, **39**, 18–42.

Plint, A.G., Norris, B. and Donaldson, W.S. 1990. Revised definitions for the Upper Cretaceous Bad Heart Formation and associated units in the Foothills and Plains of Alberta and British Columbia. *Bulletin of Canadian Petroleum Geology*, **38**, 78–88.

Plint, A.G., Tyagi, A., McCausland, P.J.A., Krawetz, J.R., Zhang, H., Roca, X., Hu, Y.G., Varban, B.L., Kreitner, M.A. and Hay, M.J. 2012a. Dynamic relationship between subsidence, sedimentation, and unconformities in mid-Cretaceous, shallow-marine strata of the Western Canada Foreland Basin: Links to Cordilleran Tectonics. In: Busby, C. and Azor Pérez, A. (Eds), Recent Advances in the Tectonics of Sedimentary Basins, 480–507. Wiley-Blackwell Publishing Ltd.; Oxford, U.K.

Plint, A.G., Uličný, D., Čech, S., Walaszczyk, I., Gröcke, D.R., Laurin, J., Shank, J.A. and Jarvis, I. 2022. Trans-Atlantic correlation of Late Cretaceous high-frequency sea-level cycles. *Earth and Planetary Science Letters*, **578**, 117323.

Plint, A.G. and Wadsworth, J.A. 2006. Delta plain paleodrainage patterns reflect small-scale fault movement and subtle forebulge uplift: Upper Cretaceous Dunvegan Formation, Western Canada Foreland Basin. In: Dalrymple, R.W., Leckie, D.A. and Tillman, R.W. (Eds), Incised-Valley Systems in Time and Space. *Society of Economic Paleontologists and Mineralogists, Special Publication*, **85**, 219–237.

Plint, A.G. and Walker, R.G. 1987. Morphology and origin of an erosion surface cut into the Bad Heart Formation during major sea level change, Santonian of west-central Alberta. *Journal of Sedimentary Petrology*, **57**, 639–650.

Plint, A.G., Walker, R.G. and Bergman, K.M. 1986. Cardium Formation 6. Stratigraphic framework of the Cardium in subsurface. *Bulletin of Canadian Petroleum Geology*, **34**, 213–225.

Potter, P.E., Maynard, W.A. and Pryor, W.A. 1980. Sedimentology of shale, 310 pp. Springer-Verlag; New York.

Price, R.A. 1994. Chapter 2. Cordilleran tectonics and the evolution of the Western Canada Sedimentary basin. In: Mossop, G. and Shetson, I. (Compilers), Geological Atlas of the Western Canada Sedimentary Basin, 13–24. Canadian Society of Petroleum Geologists and Alberta Geological Survey; Calgary.

Raines, M.K., Hubbard, S.M., Kukulski, R.B., Leier, A.L. and Gehrels, G.E. 2013. Sediment dispersal in an evolving foreland: Detrital zircon geochronology from the Upper Jurassic and lowermost Cretaceous strata, Alberta Basin, Canada. *Geological Society of America, Bulletin*, **125**, 741–755.

Ricketts, B.D. 2019. Cordilleran sedimentary basins of western Canada record 180 million years of terrane accretion. In: Miall, A.D. (Ed.), The sedimentary basins of the United States and Canada (2nd Ed.), 445–475. Elsevier; Amsterdam.

Roca, X., Rylaarsdam, J.R., Zhang, H., Varban, B.L., Sisulak, C.F., Bastedo, K. and Plint, A.G. 2008. An allostratigraphic correlation of Lower Colorado Group (Albian) and equivalent strata in Alberta and British Columbia, and Cenomanian rocks of the Upper Colorado Group in southern Alberta. *Bulletin of Canadian Petroleum Geology*, **56**, 259–299.

Ross, G.M. and Eaton, D.W. 1999. Basement reactivation in the Alberta Basin: Observational constraints and mechanical rationale. *Bulletin of Canadian Petroleum Geology*, **47**, 391–411.

Ross, G.M. and Eaton, D.W. 2001. Reply to Discussion on Basement reactivation in the Alberta Basin: Observational constraints and mechanical rationale. *Bulletin of Canadian Petroleum Geology*, **49**, 429–433.

Ross, G.M., Milkereit, B., Eaton, D., White, D., Kanasewich, E.R. and Burianyk, M.J.A. 1995. Paleoproterozoic collisional orogen beneath the western Canada sedimentary basin imaged by Lithoprobe crustal seismic-reflection data. *Geology*, **23**, 195–199.

Ross, G.M., Parrish, R.R., Villeneuve, M.E., and Bowring, S.A. 1991. Geophysics and geochronology of the crystalline basement of the Alberta Basin, Western Canada. *Canadian Journal of Earth Sciences*, **28**, 512–522.

Schieber, J. 1994. Evidence for high-energy events and shallow-water deposition in the Chattanooga Shale, Devonian, central Tennessee, USA. *Sedimentary Geology*, **93**, 193–208.

Schieber, J. 2016. Mud re-distribution in epicontinental basins – exploring likely processes. *Marine and Petroleum Geology*, **71**, 119–133.

Schieber, J., Southard, J. and Thaisen, K. 2007. Accretion of mudstone beds from migrating floccule ripples. *Science*, **318**, 1760–1763.

Schlüter, C. 1877. Kreide-Bivalven. Zur gattung *Inoceramus*. *Palaeontographica*, **24**, 249–288.

Schultz, S.K., MacEachern, J.A. and Gibson, H.D. 2019. Late Mesozoic reactivation of Precambrian structures and their resulting effects on the sequence stratigraphic architecture of the Viking Formation of east-central Alberta, Canada. *Lithosphere*, **11**, 308–321.

Schwartz, R.K. and DeCelles, P.G. 1988. Cordilleran foreland basin evolution in response to interactive Cretaceous thrusting and foreland partitioning, southwestern Montana. In: Schmidt, C.J. and Perry, W.J. (Eds), Interaction of the Rocky Mountain foreland and the Cordilleran thrust belt. *Geological Society of America, Memoir*, **171**, 489–513.

Shank, J.A. and Plint, A.G. 2013. Allostratigraphy of the Upper Cretaceous Cardium Formation in subsurface and outcrop in southern Alberta, and correlation to equivalent strata in northwestern Montana. *Bulletin of Canadian Petroleum Geology*, **61**, 1–40.

Shurr, G.W. and Rice, D.D. 1986. Paleotectonic controls on deposition of the Niobrara Formation, Eagle Sandstone, and equivalent rocks (Upper Cretaceous), Montana and South Dakota. In: Peterson, J.A. (Ed.), Paleotectonics and sedimentation in the Rocky Mountain region, United States. *American Association of Petroleum Geologists, Memoir*, **41**, 193–211.

Stott, D.F. 1963. The Cretaceous Alberta Group and equivalent rocks, Rocky Mountain Foothills, Alberta. *Geological Survey of Canada, Memoir*, **317**, 306 pp.

Stott, D.F. 1967. The Cretaceous Smoky Group, Rocky Mountain Foothills, Alberta and British Columbia. *Geological Survey of Canada, Bulletin*, **132**, 133 pp.

Vakarelov, B.K. and Bhattacharya, J.P. 2009. Local tectonic control on parasequence architecture: Second Frontier sandstone, Powder River Basin, Wyoming. *American Association of Petroleum Geologists, Bulletin*, **93**, 295–327.

Vakarelov, B.K., Bhattacharya, J.P. and Nebrigic, D.D. 2006. Importance of high-frequency tectonic sequences during greenhouse times of Earth history. *Geology*, **34**, 797–800.

Varban, B.L. and Plint, A.G. 2008. Palaeoenvironments, palaeogeography, and physiography of a large, shallow, muddy ramp: Late Cenomanian–Turonian Kaskapau Formation, Western Canada foreland basin. *Sedimentology*, **55**, 201–233.

Villeneuve, M.E., Ross, G.M., Parrish, R.R., Thériault, R.J., Miles, W., and Broome, J. 1993. Geophysical subdivision, U-Pb geochronology and Sm-Nd isotope geochemistry of the crystalline basement of the Western Canada Sedimentary Basin, Alberta and northeastern British Columbia. *Geological Survey of Canada, Bulletin*, **477**, 86 pp.

Wadsworth, J.A. and Walker, R.G. 1991. Morphology and origin of erosion surfaces in the Cardium Formation (Upper Cretaceous, Western Interior Seaway, Alberta) and their implications for rapid sea level fluctuations. *Canadian Journal of Earth Sciences*, **28**, 1507–1520.

Walaszczyk, I., Plint, A.G. and Landman, N.H. 2017. Inoceramid bivalves from the Coniacian and basal Santonian (Upper Cretaceous) of the Western Canada Foreland Basin. *Bulletin of the American Museum of Natural History*, **414**, 53–103.

Williams, G.D. and Stelck, C.R. 1975. Speculations on the Cretaceous palaeogeography of North America. In: Caldwell, W.G.E. (Ed.). The Cretaceous System in the Western Interior of North America. *Geological Association of Canada, Special Paper*, **13**, 1–20.

Wright, G.N., McMechan, M.E. and Potter, D.E.G. 1994. Chapter 3, Structure and architecture of the Western Canada Sedimentary Basin. In: Mossop, G. and Shetsen, I. (Compilers), Geological Atlas of the Western Canada Sedimentary Basin, 25–40. Canadian Society of Petroleum Geologists and Alberta Research Council; Calgary.

Manuscript submitted: 21st February 2023
Revised version accepted: 19th June 2023